Mafic Volcanism and Environmental Geology of the Eastern Snake River Plain, Idaho

Scott S. Hughes
Department of Geology, Idaho State University, Pocatello, ID 83209
Richard P. Smith
Idaho National Engineering and Environmental Laboratory, P.O. Box 1625, M.S. 2107, Idaho Falls, ID 83403
William R. Hackett
WRH Associates, Salt Lake City, UT 84117
Steven R. Anderson
U.S. Geological Survey, INEEL Project Office, Idaho Falls, ID 83403

ABSTRACT

Geology presented in this field guide covers a wide spectrum of internal and surficial processes of the eastern Snake River Plain, one of the largest components of the combined late Cenozoic igneous provinces of the western United States. Focus is on Quaternary basaltic plains volcanism that produced monogenetic coalescent shields, and phreatomagmatic eruptive centers that produced tuff cones and rings. These dominant systems are compared to compositionally evolved polygenetic eruptive centers and silicic domes that represent an extended range of petrologic processes. Selected non-volcanic features are included to illustrate the importance of stream runoff, eolian sediment, the Snake River Plain aquifer and seasonal fires on the ecology of this region. The guide is constructed in two parts, beginning with an overview of the geology followed by road directions, with explanations, for specific locations and possible side trips. The geology overview section briefly summarizes the collective knowledge gained, and implications made, over the past few decades. The road guide mainly covers plains volcanism, lava flow emplacement, basaltic shield growth, phreatomagmatic eruptions, and complex eruptive centers. Locations and explanations are also provided for environmental topics associated with the region, such as geohydrology, groundwater contamination, range fires and cataclysmic floods.

INTRODUCTION

The eastern Snake River Plain (ESRP) is an east-northeast-trending 600-km long, 100-km wide topographic depression extending from Twin Falls to Ashton, Idaho. Corporate agriculture, especially potatoes, grains and sugar beets, is the dominant economy supported by a vast groundwater and surface water system. The Idaho National Engineering and Environmental Laboratory (INEEL), a U.S. Department of Energy nuclear facility, covers 2,315 km^2 of the ESRP. Much of the remaining rangeland, including that which is covered by relatively fresh lava flows, is controlled by the U.S. Bureau of Land Management. The terrain is semiarid steppe developed on eolian and lacustrine soils that variably cover broad expanses of basaltic lava. The ESRP is bounded on the north and south by mountains and valleys associated with the Basin-and-Range province. These mountains trend perpendicular to the axis of the Snake River Plain.

Several major late Tertiary geologic events are important to the formation of the ESRP. These include: (1) time-transgressive Miocene-Pliocene rhyolitic volcanism associated with the track of the Yellowstone hotspot, (2) Miocene to Recent crustal extension which produced the Basin-and-Range province, (3) Quaternary outpourings of basaltic lavas and construction of coalescent shield volcanoes, and (4) Quaternary glaciation and associated eolian, fluvial, and lacustrine sedimentation and catastrophic flooding. Environmental issues on the ESRP and surroundings include natural hazards related to these events plus the availability of clean groundwater and the migration of industrial pollutants. An almost yearly occurrence of range fires with concomitant dust storms constitutes an additional geomorphic factor.

This field trip guide is an updated version of an earlier publication (Hughes et al., 1997c), and covers selected aspects of volcanism and associated surface and subsurface processes. Previ-

Hughes, S.S., Smith, R.P., Hackett, W.R., and Anderson, S.R.,1999, Mafic Volcanism and Environmental Geology of the Eastern Snake River Plain, Idaho, *in* Hughes, S.S., and Thackray, G.D., eds., Guidebook to the Geology of Eastern Idaho: Idaho Museum of Natural History, p. 143-168.

ous studies of ESRP basaltic magmatism and surficial processes provide the geologic basis for this article (e.g. Stearns et al., 1938; Prinz, 1970; various chapters in Greeley and King, 1977; Greeley, 1982; Kuntz et al., 1982, 1986a, 1986b, 1992, 1994; Malde, 1991; Pierce and Morgan, 1992; and many others). Published ESRP field guides include those by Greeley and King which presented ESRP volcanism as a terrestrial planetary analogue; Hackett and Morgan (1988) which dealt with explosive volcanism and focused on emplacement of rhyolite ash-flow sequences; Kuntz (1989) which concentrated on Craters of the Moon; and Hackett and Smith (1992) which dealt mainly with geology of the INEEL and surroundings. General aspects of ESRP geology are presented here, emphasizing the emplacement of non-explosive basaltic dikes and lavas, their compositions, and phreatomagmatic basaltic eruptions that are directly related to proximity of magmatism to the Snake River or Pleistocene lakes. Readers should refer to the guides mentioned above for more in-depth treatment of their respective topics.

The field trip plan is constructed around logistics of travel throughout the ESRP, rather than topics, because the locations of various styles of volcanism are spatially intermixed. We have attempted to limit the inevitable overlap with other field trip guides to features that would be important to first-time visitors as well as seasoned ESRP geologists.

GEOLOGIC SETTING

Quaternary volcanic landforms, i.e., basaltic lava flows, shield volcanoes, and rhyolitic domes, dominate the physiography of the ESRP (Figs. 1 and 2). Numerous basaltic lava fields form a commingled volcanic sequence with intercalated sediment in the

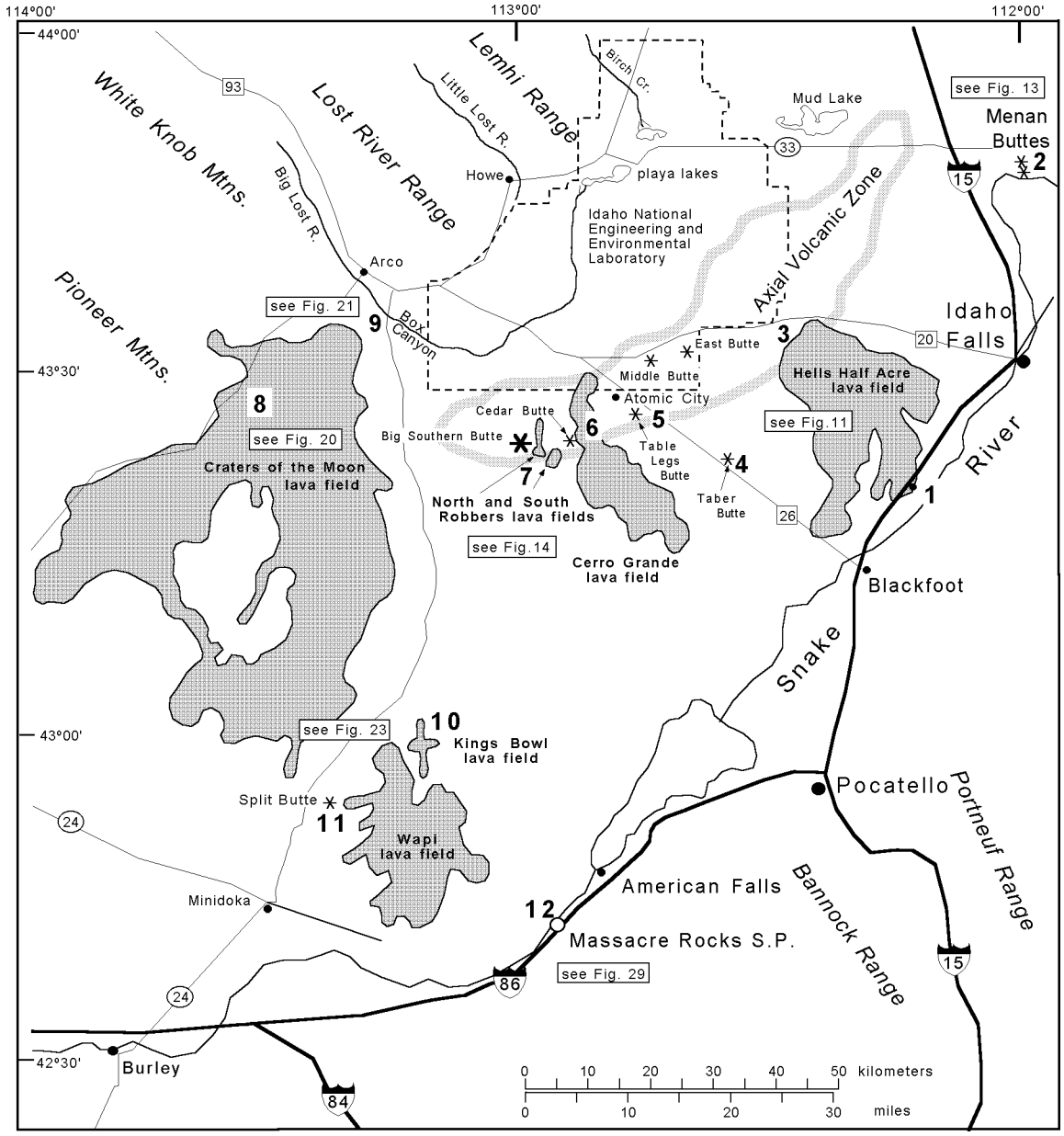

Figure 1. Map of the field trip area showing the location of the axial volcanic zone in relation to the latest Pleistocene-Holocene basaltic lava fields (shaded fields). Field trip stops are shown in boldface numbers. Refer to figure numbers in boxes for detailed figures and road maps.

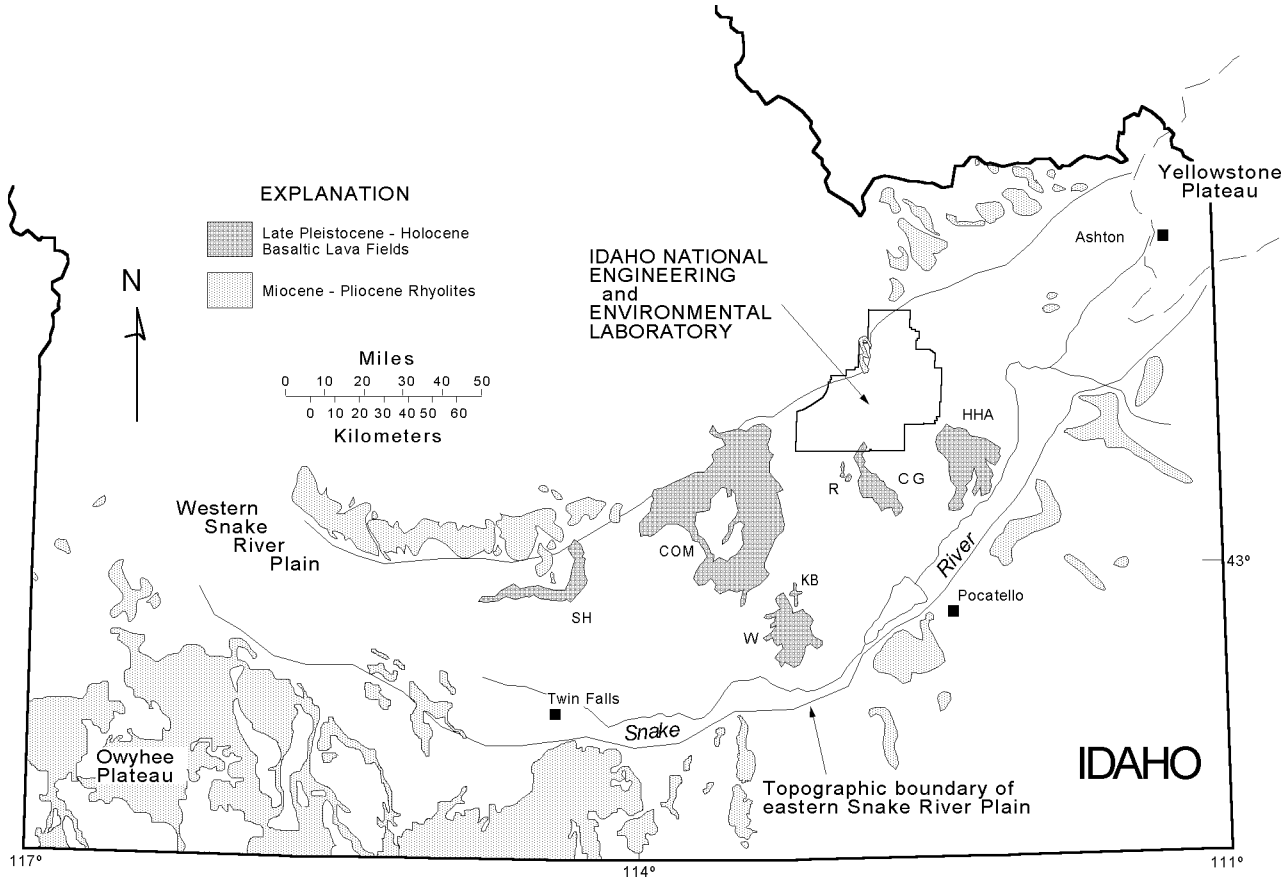

Figure 2. Map of southern Idaho with the locations of Owyhee Plateau, Yellowstone Plateau, Idaho National Engineering and Environmental Laboratory (INEEL), latest Pleistocene-Holocene basaltic lava fields (dark shading), and major outcrops of Miocene-Pliocene rhyolites. Abbreviations for lava fields are: SH = Shoshone, COM = Craters of the Moon, W = Wapi, KB = Kings Bowl, R = North and South Robbers, CG = Cerro Grande, and HHA = Hells Half Acre.

upper 1-2 km of the crust. Less common are compositionally complex eruptive centers comprised of pyroclastic cones, dikes, and chemically evolved lavas. Domes (Fig. 3), shields (Fig. 4) and complex eruptive centers are concentrated along a proposed northeast-trending axial volcanic zone (Stops 4-8) which constitutes the topographically high central axis of the ESRP (Hackett and Smith, 1992; Kuntz et al., 1992). A relatively high density of eruptive centers southwest of the axial volcanic zone and diversion of surface drainage (the Big Lost River turns northward as it enters the plain) by volcanic topography lead to the suggestion that the axial zone extends farther to the southwest to include Craters of the Moon. Basalts typically erupt from fissures located along, and subparallel to, NW-SE volcanic rift zones that parallel Basin-and-Range structures in southern Idaho. Miocene-Pliocene rhyolitic ash-flow tuffs lie beneath the basaltic cover and are exposed in ranges along the margins of the ESRP (Fig. 2). These older rhyolitic caldera eruptions are associated with time-transgressive volcanism from SW Idaho at ~14 Ma to Yellowstone National Park at 2-0.6 Ma (Pierce and Morgan, 1992).

Widespread basaltic volcanic activity occurred intermittently on the ESRP throughout Pleistocene and Holocene time. Kuntz et al. (1992) estimate a meager magma output rate of 3.3 km^3 per 1000 years for the entire ESRP during the past 15,000 years. Thickness of most individual basalt flows in the upper part of the volcanic section ranges from about 5 m to as much as 25 m, and the flows extend up to 48 km. The lavas are predominantly diktytaxitic olivine tholeiites emplaced as channel or tube-fed pahoehoe flows from fissures associated with small monogenetic shield volcanoes (Stop 5). Petrologic studies (Leeman, 1982b; Leeman et al., 1976) indicate that ESRP basaltic lavas range from primary olivine tholeiites to evolved (fractionated and/or contaminated) compositions, the latter of which are associated with polygenetic centers.

Many individual lava flow units contribute to the growth of each shield over a few months or years. Seven monogenetic basaltic volcanic fields have formed since ~12 ka (Fig. 2). These include the Shoshone, Wapi, Kings Bowl (Stop 10), North Robbers (Stop 7), South Robbers, Cerro Grande (Stop 6), and Hells Half Acre (Stops 1 and 3) lava fields that cover approximately 13 percent of the ESRP. Craters of the Moon volcanic field (Stop 8) represents a polygenetic, compositionally evolved system comprising several individual eruptive centers active from 15 to 2 ka. Basaltic tuff cones such as the impressive Menan Buttes (Stop 2) and the Massacre Volcanic Complex (Stop 12) prevail at hydromagmatic eruptive centers proximal to the Snake River; however, these types of volcanoes are more prevalent downstream, between Twin Falls and Boise in the western Snake River Plain province (McCurry et al., 1997). Tuff rings such as Split Butte (Stop 11) are uncommon on the ESRP and represent eruptions into saturated ground beneath transient lakes or other regions with

Figure 3. View from East Butte looking west: Middle Butte (foreground, ~7 km distant) and Big Southern Butte (~30 km distant) rhyolitic domes on the eastern Snake River Plain. Middle Butte is a cryptodome covered by Quaternary basaltic lavas that were uplifted during emplacement.

elevated water tables. For example, phreatic eruptions near Mud Lake (Fig. 1) produced mixed volcaniclastic deposits of sand, ash and juvenile scoria containing numerous accidental blocks of lacustrine sediment and older basalt.

Basaltic shields topographically control the deposition of younger sediments and lavas (Hughes et al., 1997a). Modern sediments are distributed on the ESRP largely in eolian, lacustrine (playa-like "sinks") and fluvial depositional systems (e.g. Hackett and Smith, 1992; Kuntz et al., 1992, 1994; Geslin et al., 1997; Gianniny et al., 1997). Playa sediments are clay-rich silt and fine-sand mixtures of eolian and stream-born material. Fluvial sediments are mostly coarser sand, pebbles and cobbles. North of the axial volcanic zone they are derived from the Big Lost River, Little Lost River, and Birch Creek drainages with outlets on the INEEL. South of the axial volcanic zone fluvial sediments are controlled by the Snake River and its tributaries, the Henrys Fork, Blackfoot and Portneuf rivers. Loess and eolian sand also covers most pre-Holocene surfaces and occurs as layers between lava flow groups in the subsurface.

BIMODAL VOLCANISM ON THE EASTERN SNAKE RIVER PLAIN

The Yellowstone Hotspot

Volcanism associated with the Snake River Plain in Idaho and adjacent areas of Nevada and the Yellowstone plateau during the past 16 Ma is the manifestation of a bimodal (rhyolitic/basaltic) continental tectono-magmatic system. The Yellowstone-Snake River Plain volcanic system is largely made up of thick, time-transgressive rhyolitic ignimbrites and lavas probably caused by melting above a mantle hotspot (Pierce and Morgan, 1992; Smith and Braile, 1994). Age-progressive rhyolites are mainly exposed along the northern and southern boundaries of the ESRP, on the Yellowstone Plateau, and on the Owyhee Plateau of southwestern Idaho (Fig. 2).

Hypotheses invoked to explain this age progression recognized by Armstrong et al. (1975) include: (1) the trace of a stationary deep-seated mantle plume, currently beneath the northeast part of Yellowstone National Park (Morgan, 1972; Smith and Sbar, 1974); (2) an eastward propagating rift in the lithosphere, which caused melting of the asthenosphere by decompression (Myers and Hamilton, 1964; Hamilton, 1989); (3) volcanism along a preexisting crustal flaw (Eaton et al., 1975); (4) propagation of a crack following a transform fault boundary between two regimes of Basin-and-Range extension (Christiansen and McKee, 1978); and (5) a meteorite impact which initiated the eruption of large volumes of flood basalts (Alt et al., 1988). The most widely accepted hypothesis is that the ESRP was formed above a hotspot track, created by the passage of the North American plate southwestward over a stationary mantle plume (Armstrong et al., 1975; Leeman, 1982a; Pierce and Morgan, 1992; Smith and Braile, 1994). The true nature of the hotspot is unknown; thus the origin, dimensions and tectonic association of the purported plume are subjects for continued geologic investigation.

Late Tertiary bimodal magmatism associated with the incep-

Figure 4. Wapi lava field, view from the northeast, illustrating the low profile typical of monogenetic basaltic shields on the eastern Snake River Plain. Pillar Butte, the prominent peak located near the southern edge of the eruptive center, is approximately 5 km away.

tion of the Yellowstone hotspot track reflects a complex tectonic system involving the Columbia Plateau, Oregon Plateau, Owyhee Plateau, and Snake River Plain (e.g. Christiansen and McKee, 1978; Richards et al., 1989; Pierce and Morgan, 1992; Smith and Braile, 1994). The relative volcanic ages and positions of these regions are possibly associated with northward deflection of a rising mantle plume at ~20 Ma by the subducting Farallon plate (Geist and Richards, 1993). According to their model, the downgoing slab was subsequently penetrated at ~17.5 Ma and allowed the plume to pass through to produce the Columbia River Basalt and the Yellowstone hotspot track. Camp (1995) suggests that the north-northwest alignment of mid-Miocene volcanism along the Nevada-Oregon rift zone resulted from compression and distortion of the plume head against the cratonic margin of North America between 17 and 14 Ma. His model allows for a spread in volcanic activity away from the center of the plume and a southward shift in volcanism at ~14 Ma as the distorted plume crest was overridden by Precambrian crust.

Estimated rates of southwestward movement of the North American continental plate range from 2.9-7 cm/yr. Pierce and Morgan (1992) indicate a shift in the hotspot track near Twin Falls that relates to decrease in rate of hotspot migration (7 cm/yr to 2.9 cm/yr) and change in direction (N70-75°E to N54°E). Accounting for Basin-and-Range extension along the hotspot track and Miocene-Pliocene plate rotation, Rodgers et al. (1990) determined a rate of 4.5 cm/yr and a direction of N56°E of the volcanic track over the last 16 Ma. Therefore, the present position of the hotspot is possibly 90 km northeast of the oldest Yellowstone caldera.

Basaltic Plains Volcanism

Time-space relations of rhyolite and basalt are dissimilar. Although the inception of ESRP basaltic volcanism exhibits a general time-progressive trend (Armstrong et al., 1975), Pleistocene-Holocene lavas occur over much of the ESRP. Up to 2 km of late Tertiary, Quaternary and Holocene diktytaxitic olivine tholeiite lavas covered the ESRP and lie above the Miocene-Pliocene rhyolites. Detailed surface maps by Kuntz (1979) and Kuntz et al. (1988, 1994), along with investigations into mechanisms of basaltic magmatism (Kuntz, 1992; Kuntz et al. 1982, 1986a, 1992) have lead to models of the magmatic sources and lithospheric plumbing systems. Well-exposed volcanic vents, as well as eruptive and non-eruptive fissure systems visible in and around some Holocene lava fields, occur mainly along the northwest-southeast volcanic rifts zones.

Many of the ESRP volcanic landforms and eruptive mechanisms were described in Greeley and King (1977) and later in Greeley (1982), both of which developed the concept of basaltic "plains-style volcanism". Low-profile basaltic shields on the ESRP (Fig. 4) produce subdued topography and shallow depositional slopes. Most shields are formed by low-volume monogenetic eruptions over short time spans, so they have little opportunity for significant growth above the surrounding topographic surface. Interspersed among shields are middle Pleistocene rhyolite domes (Fig. 3), such as Big Southern Butte, Middle Butte and East Butte, which stand out in isolated grandeur (Stop 4) on the relatively flat basaltic plain. Complex volcanic centers, such as Cedar Butte (McCurry et al., 1999, this volume) and Craters of the Moon (Stop 8), exhibit intermediate to silicic magma spanning the "bimodal" gap. ESRP volcanic stratigraphy is, therefore, a complex Quaternary-Holocene succession that includes small coalescent shields, tuff rings and cones, evolved eruptive centers with composite cones, rhyolite domes, and sedimentary interbeds (Fig. 5).

Vent regions exhibit either spatter ramparts, which are positive topographic features, or broad collapse pits where lavas flowed through a breached portion of the shield. Lava flow sequences are readily observed in the walls of breached summits, as evident at Black Butte Crater in the Shoshone lava field which produced an impressive 48 km-long tube-fed basaltic lava flow (Fig. 2). Lava lakes form in vent areas during the release of lava into tube-fed or channel-fed flow systems. Their presence is evident in young vent systems that are not obscured by loess, such as the Pillar Butte eruptive center of the Wapi lava field (Fig. 6) which has a radiocarbon age of 2,270 ± 50 B.P. (Kuntz et al., 1986b). Lava lakes are evident in many other late Pleistocene and Holocene vent areas although they are variably obscured by eolian deposits.

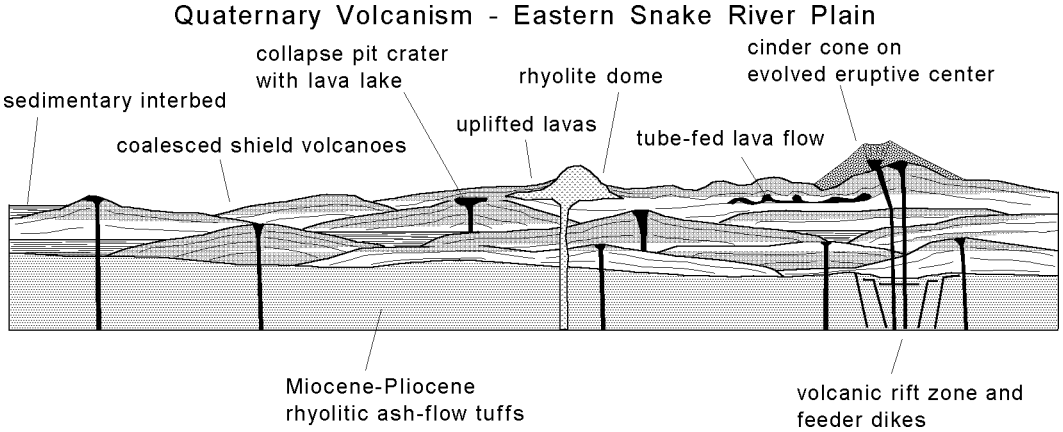

Figure 5. Schematic diagram of plains volcanism on the eastern Snake River Plain. Modified from Greeley (1977), the diagram illustrates myriad magmatic and surficial processes that contribute to the evolution of the province.

Figure 6. East flank of Pillar Butte, the eruptive spatter and block vent for the Holocene Wapi lava field, is partially surrounded by a lava lake produced during collapse and infilling of the vent area.

Tectonic Influences on Basaltic Magmatism

Dike Injection

Mechanisms of magma storage, dike injection and eruption, invoked from previous investigations and comparative detailed studies of other basaltic systems, allow some speculation of the tectonic influences on ESRP magmatism. Volcanic rift zones on the ESRP are manifested by linear sequences of basaltic vents with associated fissure-fed flows and open fissures that are generally parallel to, but not collinear with, Basin-and-Range faults north and south of the plain (Kuntz et al., 1992). Locations of known eruptive centers (Kuntz et al., 1994) and inferred subsurface eruptive centers (Wetmore, 1998) do not predict distinct, narrow rift systems; rather, they indicate broader zones of extensional strain accommodation and numerous small "vent corridors" as suggested by one of us (Anderson). Surface deformation near eruptive centers includes linear fractures, grabens and monoclines due to shallow magma injection. Orientation of inferred basaltic feeder dikes, evidenced by the alignments of surface deformation features and vents, suggests that they reflect, at least in part, a regional southwest-northeast extension corresponding to the direction of least-compressive stress.

Tectonic extension on the ESRP is believed to be accommodated more by dike injection than faulting (Hackett and Smith, 1992), although in the Basin-and-Range province the lithosphere extends by normal faulting. Regional stress apparently affects basaltic magma emplacement in reservoirs in the upper mantle or lower crust where primary melts accumulate above the region of partial melting. Kuntz's (1992) magmatic model suggests that basaltic magma is stored beneath ESRP eruptive centers in narrow elongate sill and dike networks perpendicular to the direction of least-compressive stress. Fracture systems related to regional horizontal extension allow magmas to locally penetrate all levels of the lower and middle crust along a vertically-oriented dike system.

This scenario implies that ESRP extension-related magmatism is comparable to that measured or inferred at active basalt rift systems although the mechanisms of extension may differ somewhat. Dikes in Hawai'i and Iceland are emplaced as blade-like structures propagating laterally from a magma reservoir (Rubin and Pollard, 1987) as the crust is inflated and extended around the chamber. Whether or not an eruption ensues, fissures may form on the surface if dikes are sufficiently shallow. A horizontal component of magma injection, whereby magma migrates along the length of a fissure during or prior to vertical ascent, may occur in some dikes associated with rift zones on the ESRP. Non-eruptive fissures and grabens that extend beyond the edges of Holocene volcanic fields and away from their eruptive centers (Kuntz et al., 1988, 1994) may be related to lateral dike propagation away from the eruptive part of the fissure as well as vertical dike propagation above the reservoir.

Figure 7 depicts the general scenario of ESRP dike and reservoir geometry based on the perspectives of Rubin and Pollard (1987), Kuntz (1992), and Hackett and Smith (1992). Lateral magma migration in a blade-like fashion is highly speculative, considering the lack of large Hawaiian-type shields capable of magma storage above the surrounding topographic surface. However, surface features observed on the ESRP could result from variable amounts of magma ascent and spreading from a tabular reservoir. As a dike ascends into overlying basaltic layers, the

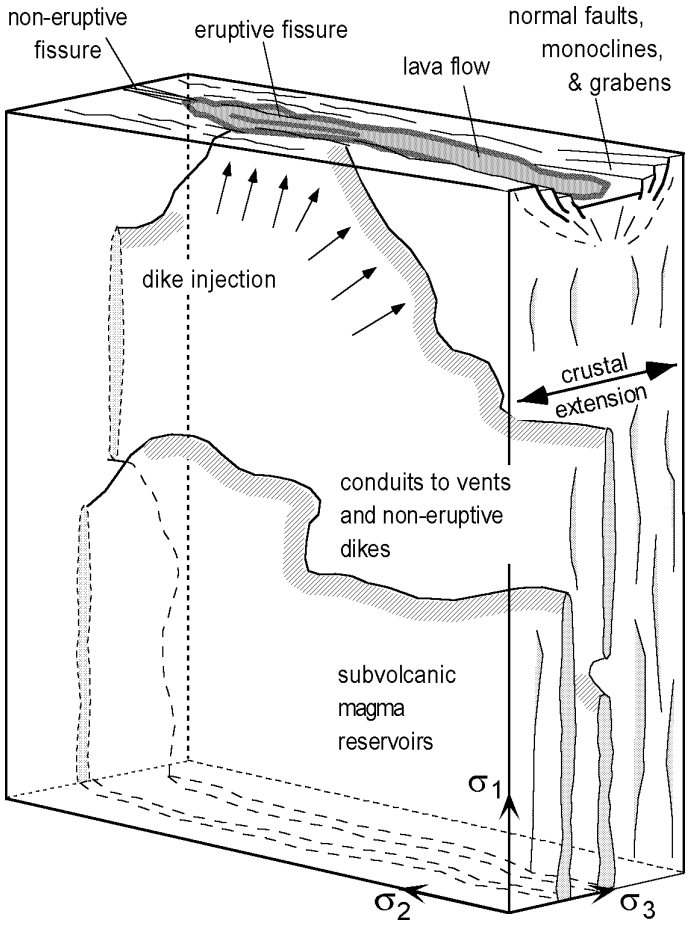

Figure 7. Schematic model of dike emplacement on the eastern Snake River Plain and the relation to surface deformational features. Propagation is possible when the fracture toughness of the country rock is exceeded by magma pressure. Orientation of dikes and vertical reservoirs are controlled by the regional stress field. Adapted from Rubin and Pollard, 1987; Kuntz, 1992; and Hackett and Smith, 1992.

extension above the advancing dike produces nested grabens providing low topographic areas for lava accumulation as magma erupts on the surface. Lava partially or wholly covers the depressed region as it flows over non-eruptive segments of the fissure system.

Perhaps the most important factor in the style of ESRP magmatism, and its dependency on crustal extension, is a relatively low magma supply rate which is manifested in numerous small monogenetic eruptive centers rather than large complex shields. Compared to regions of high magma production rates, such as Hawai'i or Iceland where shield tumescence due to magma injection is followed by deflation during an eruption, ESRP subsurface reservoirs do not have significant readjustment during an eruption. This results in short-lived low-volume eruptions because a progressive pressure drop occurs as the reservoir is depleted (Kuntz, 1992). ESRP eruptions terminate at a critical pressure level a relatively short time after the eruption begins.

Chemical Variations

Tectonic influences are also reflected in chemical compositional variations in ESRP volcanic rocks, which are erupted in a within-plate tectonic province. The system has been described as being "bimodal" (rhyolite and basalt), yet there are clearly intermediate compositions. Major element chemical trends (Fig. 8a and b) demonstrate that the evolved eruptive centers produce a wide range in compositions without significant break between end-members. Detailed discussions of ESRP petrology (e.g. Leeman, 1982b; Leeman et al., 1976, 1985; Kuntz et al., 1992) indicate complex processes related to source heterogeneity, fractionation of primary magmas, and crustal assimilation that are responsible for the diversity among ESRP volcanic rocks. Intermediate chemical and lithologic compositions are found in evolved eruptive centers such as Cedar Butte volcano (McCurry et al., this volume) and Craters of the Moon lava field (Stop 8).

Compared to these evolved compositions, olivine tholeiite chemical signatures fall in a tighter cluster that initially suggests uniformity in magma genesis and evolution. However, fine-scale chemical variations are notable within and between monogenetic tholeiitic lava flow groups (Hughes et al., in press). For example, TiO_2 (~1-4 wt. %) and MgO (~3.5-12 wt. %) exhibit 3-4X variations, while similar ranges are evident in incompatible trace elements Ba, La, Hf, Zr, etc. Geochemical plots of representative flow groups sampled on the surface and in INEEL coreholes (Fig. 8c) suggest that flow groups grossly cluster into separate covariant fields. The separate chemical trends reflect individual magmatic episodes, and possible differences in source chemistry and degrees of partial melting associated with monogenetic eruptions (Hughes et al., 1997b).

The Menan Volcanic Complex

The twin cones of the Menan Buttes (Fig. 9) are part of a six-vent, late-Pleistocene complex of basaltic tuff cones and smaller tuff rings, aligned along a 5-kilometer, northwest-trending eruptive fissure west of Rexburg, Idaho. Recent work on the Menan volcanic complex includes Creighton (1982, 1987), Ferdock (1987), Hackett and Morgan (1988), and Kuntz et al. (1992).

The hydrovolcanoes of the Menan volcanic complex (Stop 3)

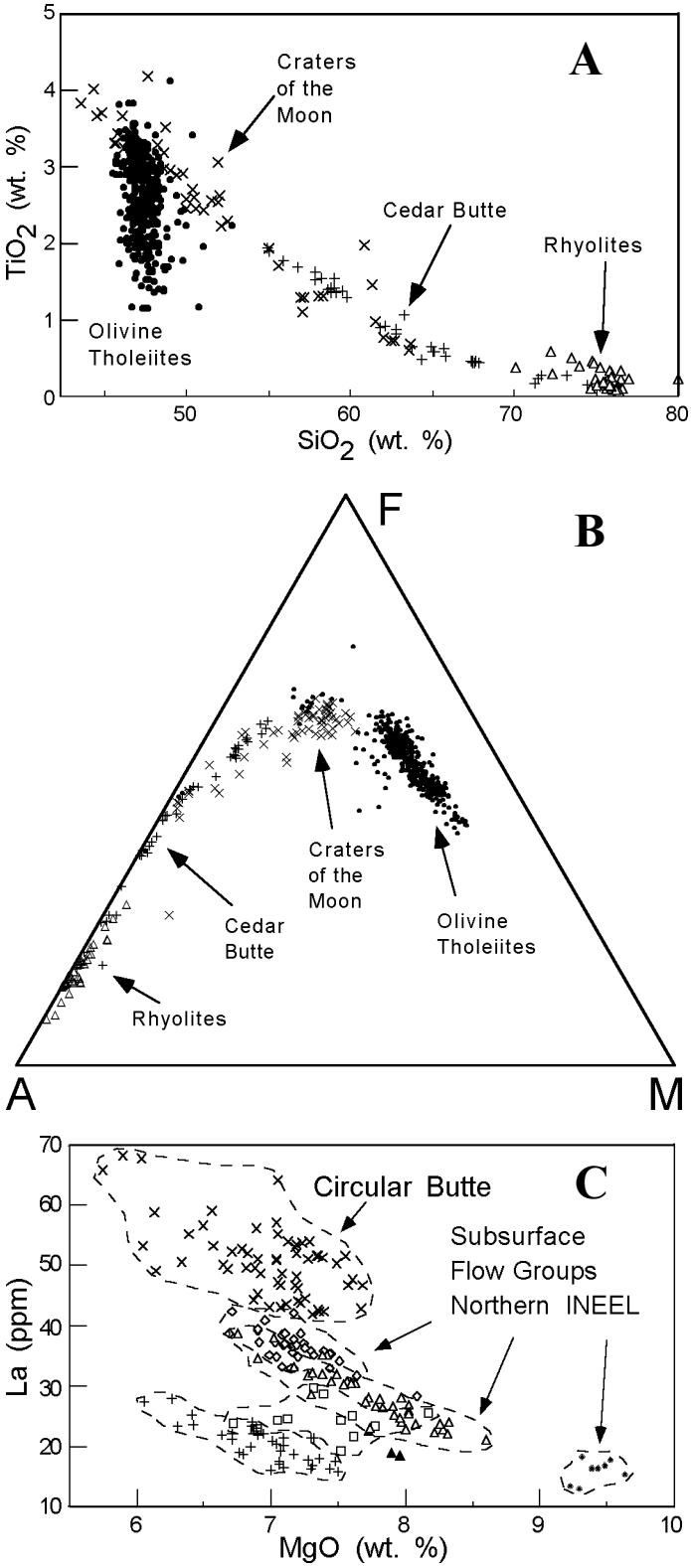

Figure 8. (a) Covariation in TiO_2 vs. SiO_2, (b) AFM (wt. % Na_2O+K_2O - FeO - MgO) diagram for ESRP compositions ranging from basalt to rhyolite, and (c) La vs. MgO plot of several flow groups sampled on the surface and in coreholes in the northern part of the INEEL. Data are from numerous sources including Leeman, 1982b,c; Kuntz et al., 1992; Hayden ,1992; Fishel, 1993; Spear, 1979; Spear and King, 1982; Leeman et al., 1985; Hildreth, et al. 1991; Stout and Nicholls, 1977; Knobel et al., 1995; Stout et al., 1994; Reed et al.,1997; and Hughes, unpublished data.

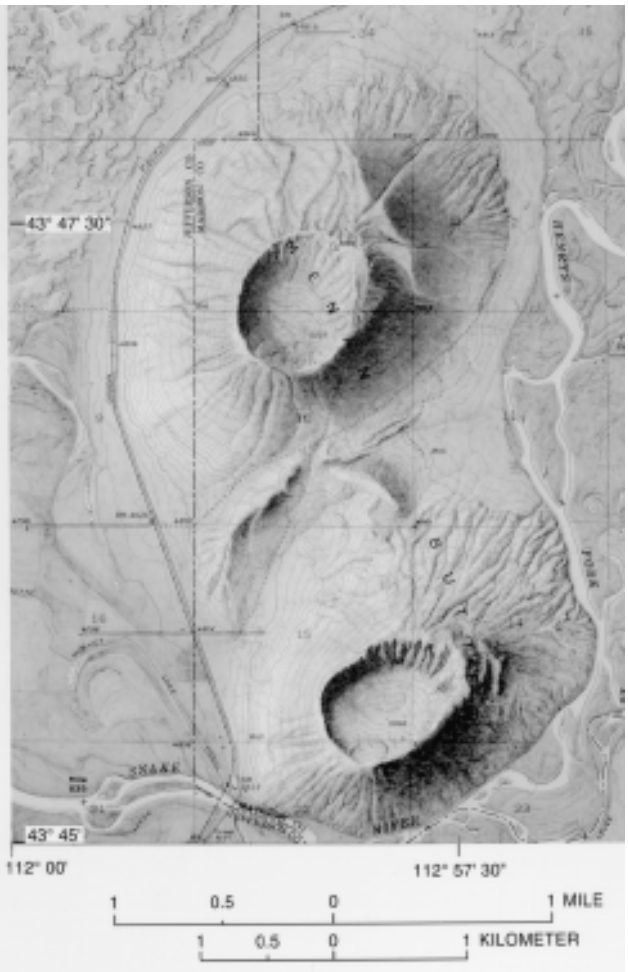

Figure 9. Portion of the Menan Buttes, Idaho shaded relief map (U.S. Geological Survey, 1951, 1:24,000 scale shaded topographic map) with large tuff cones. Phreatomagmatic eruptions occurred near the confluence of the Henrys Fork and the South Fork of the Snake River.

were formed during the ascent of a basaltic dike into near-surface, water-saturated alluvial sediment and basaltic lava flows of the Snake River Plain aquifer, producing large volumes of palagonite tuff. The north and south Menan Buttes tuff cones are the largest features of the volcanic complex, composed of massive to thin-bedded, tan, lithified palagonite lapilli tuffs containing minor accidental clasts of dense basalt and rounded quartzite pebbles. The monotonous palagonite tuffs of the Menan Buttes tuff cones are the products of steady-state hydrovolcanic eruptions of wet basaltic tephra, generated during dike emplacement into the shallow aquifer. In the later stages of cone construction, steam explosions were situated above the aquifer and within the recycled tephra-slurry of the central craters, as shown by the paucity of accidental-lithic clasts derived from the underlying alluvial sediment.

Near-vent deposits of the Menan Buttes tuff cones are massive and poorly sorted, suggesting mass emplacement as slurry flows of wet, cohesive tuff. Along the rims of the craters, original bed forms are obscured by dense palagonitization of the tephra. Cone-flank deposits are planar- and cross-stratified, moderately sorted palagonite tuffs with local armored-lapilli beds, suggesting deposition as fall, surge and sheet wash. Deformation of the wet, cohesive tuffs occurred during or soon after deposition, as shown by monoclines, complex folds and possible detached slide blocks on the lower flanks of the tuff cones. Distal deposits beyond the cone flanks are fine, planar-laminated, palagonitic fallout tuffs that were dispersed mainly to the northeast.

The North and South Little Buttes are eroded tuff rings situated along the eruptive fissure about 5 km south of the Menan Buttes. In contrast to the Menan Buttes tuff cones, the tuff rings are smaller, have lower slope angles, and the deposits are strongly cyclic with abundant quartzite pebbles derived from the underlying permeable alluvium. The cyclical nature of the eruptions is indicated by two distinctive classes of bed sets. Scoriaceous lapilli tuffs occur in coarse, planar bed sets, and were emplaced mainly as fall and minor surge deposits, during relatively "dry vent", violent strombolian eruptions. Intercalated with the scoriaceous deposits are bed sets of tan, cross-stratified, fine palagonite tuffs, emplaced as fall and surge deposits during relatively "wet vent" surtseyan eruptions, and driven largely by the flashing of external water to steam. Groundwater was probably always available during feeder-dike intrusion, and the alternating strombolian and surtseyan bed sets therefore suggest a fluctuating elevation of the magma column; such variation in magma pressure is commonly observed during historical basaltic eruptions. At the Little Buttes, vesiculating basaltic magma episodically reached the land surface, sealed itself from the incursion of external water, and erupted mainly coarse, scoriaceous ejecta. During periods of magma withdrawal, steam explosions occurred within saturated alluvium above the shallow dikes, producing fine palagonitic tuffs containing up to 50 percent quartzite clasts.

ENVIRONMENTAL GEOLOGY OF THE EASTERN SNAKE RIVER PLAIN

Earthquake and Volcanic Hazards

Geologic investigations of seismic and volcanic hazards at the INEEL have been underway for several decades. Much of the recent work has been concentrated on recent displacement on Basin-and-Range faults north of the INEEL, processes operating in volcanic rift zones within and near the INEEL, and stratigraphy and structure beneath the surface of the ESRP near INEEL. Specific investigations include paleoseismology of faults, structural geologic mapping of faults, detailed mapping of volcanic rift zones, regional geophysical surveys, high-precision geodetic surveys to measure crustal deformation, deep drilling, and heat flow analysis.

For most INEEL facilities, the seismic hazard is dominated by the Basin-and-Range normal faults north of the ESRP. These faults are capable of magnitude 7 or greater earthquakes and have recurrence intervals of thousands to tens of thousands of years. Facilities at INEEL have been designed and constructed to withstand the effects of ground motions associated with potential earthquakes on the southern ends of these faults.

The most significant volcanic hazard for INEEL facilities is inundation by lava flows, but the hazard from ground deformation (fissuring and tilting) due to shallow dike intrusion and from volcanic gases has also been evaluated (Hackett and Smith, 1994). The probability of inundation by lava flows increases towards

volcanic rift zones and the axial volcanic zone. For any particular facility the probability is less than 10-5 per year, most likely in the range of 10-6 to 10-7 per year. Impacts from ground deformation and volcanic gases are even lower. The hazard due to seismicity associated with dike intrusion and volcanism is less than the hazard due to seismicity due to tectonic processes (Smith et al., 1996). The INEEL seismic network, with stations deployed in volcanic rift zones on the ESRP and along major faults in the Basin-and-Range province, is operated to monitor tectonic seismicity and to warn of impending volcanic or intrusive activity.

Surficial Processes

Although tectonic and volcanic processes produce the gross geomorphic characteristics of the ESRP, late Pleistocene to late Holocene surficial processes, including glacial outburst flooding (Stop 9), range fires, and eolian erosion and deposition (overview at Stop 4) contribute significantly to the geomorphic appearance of the ESRP. The effects of glacial outburst flooding along the Big Lost River include scouring of loess cover from basalt lava flows, formation of large gravel bars and boulder trains, deposition of exotic gneissic and granitic boulders on basaltic terrain, excavation of cascades in basalts, and possible modifications to canyons in basalt bedrock (Rathburn, 1991, 1993).

During the Pleistocene, extensive eolian deposition produced thick loess blankets on the ESRP and in adjacent areas of southeastern Idaho (Pierce et al., 1982). Eolian processes, aided by range fire denudation of large tracts of the ESRP, have continued to modify the landscape up to the present time. Prominent lineaments on the ESRP, observed in landsat imagery and aerial photography, are the result of eolian redistribution of surficial materials following range fires (Morin-Jansen, 1987). That process has been observed in action during the last few years, and will be discussed in detail at field trip Stop 4.

Hydrogeology of the Idaho National Engineering and Environmental laboratory

Facilities at the INEEL are used in the development of peacetime atomic-energy applications, nuclear safety research, defense programs, and advanced energy concepts. Liquid radionuclide and chemical wastes generated at these facilities have been discharged to onsite infiltration ponds and disposal wells since 1952; use of disposal wells was discontinued in 1984. Liquid-waste disposal has resulted in detectable concentrations of several waste constituents in water in the Snake River Plain aquifer underlying the INEEL (Barraclough and Jensen, 1976; Bartholomay et al., 1995). Detailed stratigraphic studies using outcrops, cores, and geophysical logs are being conducted to evaluate the relations between the geologic framework and the movement of water and waste in the unsaturated zone and aquifer.

Water runoff from valleys north of the ESRP follows drainages such as the Big Lost River, Little Lost River and Birch Creek to enter an extensive groundwater system beneath the INEEL (Fig. 10). The unsaturated zone and aquifer are composed of a 500-m thick sequence of discontinuous volcanic and sedimentary deposits of Pleistocene age. Individual basalt lava flows are characterized by large zones of irregular fractures and voids (Barraclough and Jensen, 1976) creating high hydraulic conductivities. Groundwater travels southwest through the volcanic sequence and discharges mainly through highly conductive zones of basalt along the Snake River at Thousand Springs (approximately 35 km northwest of Twin Falls) which is over 200 km southwest of the recharge zone.

Stratigraphic units underlying the INEEL include mainly basalt and sediment. Basalt units, which make up about 85 percent of the volume of deposits in most areas, include individual flows, flow groups, and supergroups (Lanphere et al., 1994; Anderson et al., 1996; Welhan et al., 1997; Wetmore et al., 1997). A basalt flow group is a sequence of basalt flows such as the Hells Half Acre and Wapi lava fields that erupted within a relatively short period of time from a single fissure or series of vents related to a common magmatic system (Kuntz et al., 1980, 1994). These units represent eruption episodes that lasted from days to years. A basalt supergroup is a group of flows that cannot be separated into individual flow groups on the basis of available well data, usually because most wells involved were not cored for paleomagnetic, petrographic and geochemical studies. These units represent multiple eruptive events over thousands of years. Different amounts of intercalated lacustrine, playa, and fluvial sediment lenses and eolian soil blankets occur between flow groups and supergroups; the amount of sediments depends on both the sedimentation rate and the repose interval between eruptions at any given site.

Although many flow groups are locally separated by lenses of fine sediment ranging from a few centimeters to tens of meters in thickness, contacts between some groups apparently have little or no sediment or soil development. The overall profile of ESRP shields and the locations of vents (Figs. 4, 5 and 10) indicate control by shield construction on direction of streams and location of sedimentation (Hughes et al., 1997a). This is evident in the position of Big Lost River and Birch Creek playas in a sediment trough near TAN (Gianniny et al., 1997). The trough corresponds to an apparent paucity of eruptive shields along a northeast-southwest corridor through the INEEL (Kuntz et al., 1994, Wetmore, 1998). Volcanic vents apparently are restricted to the axial volcanic zone southeast of this corridor and along the northwest margin of the ESRP in the INEEL vicinity. Stratigraphic and lithologic studies of surface and subsurface sediments in the northern INEEL (Geslin et al., 1997) suggest that buried Pleistocene depositional environments were similar to present day playa and fluvial systems, and were controlled by volcanic topographic highs. Many of these relations will be observed and discussed at Stop 4 on the field trip.

Basaltic lava flows, as major components of the ESRP aquifer system, have internal variations in hydraulic conductivity related to their thickness and to the dimensions and orientations of scoriaceous vesiculated zones, tension fractures, brecciated rubble zones, and flow surfaces (Welhan et al., in press). These factors control conductivity on scales ranging from a few cm to several m, and the directional variances caused by them are probably random throughout a lava flow. Hydraulic conductivity varies locally over one-million fold, with highest- and lowest- conductivity zones in basaltic breccia and sedimentary interbeds, respectively. Once a shield volcano is buried by younger lavas and sediments, the orientation of the conductive brecciated zones within

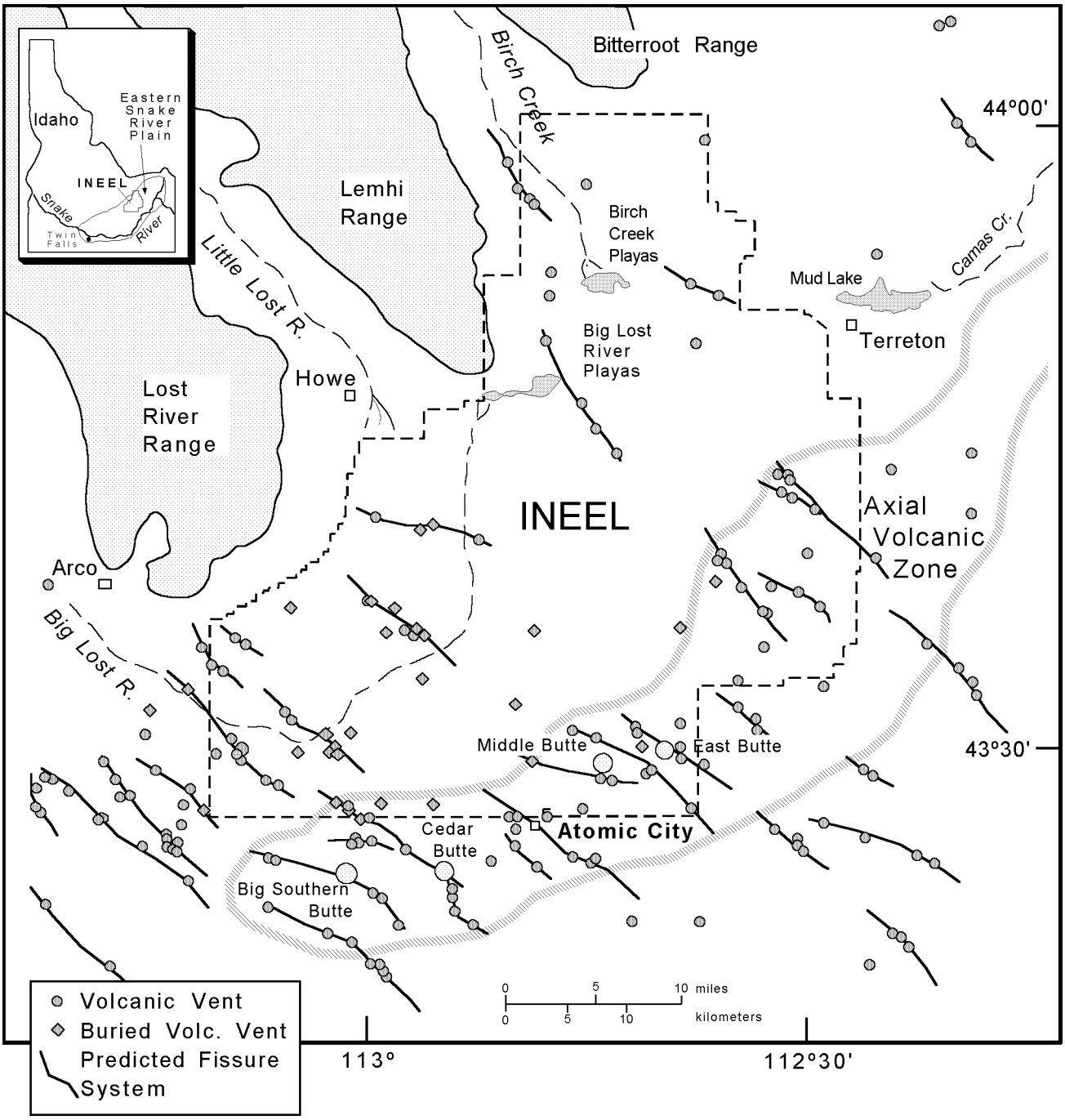

Figure 10. Map of the Idaho National Engineering and Environmental Laboratory (INEEL) on the eastern Snake River Plain. Locations are shown for exposed volcanic vents (Kuntz et al., 1994) and inferred buried eruptive centers (Wetmore, 1998) related to the axial volcanic zone and Quaternary basaltic vents. Double arrows depict hypothesized volcanic rift zones (see text for explanation).

lavas is controlled largely by the original depositional slopes. Groundwater flow is enhanced further in randomly oriented and irregular void spaces within the flow units. For example, Holocene shields, such as the Wapi and Hells Half Acre lava fields, contain a highly irregular plexus of flow channels, tubes, tumuli, collapse depressions and other surface irregularities, all of which could serve as aquifers once those shields are buried beneath the water table.

Identification and correlation of subsurface stratigraphic units rely mainly on direct and indirect measurements of basalt properties, including paleomagnetic polarity and inclination, radiometric age, petrographic characteristics, chemical compositions, and natural-gamma emissions of naturally-occurring K, U, and Th determined from borehole logging tools (Lanphere et al., 1994; Anderson and Bartholomay, 1995; Reed et al., 1997). At least 121 basalt-flow groups and 102 sedimentary interbeds have been identified at and near the INEEL (Anderson et al., 1996); however, many flow groups beyond the main facilities, where most cores and two-thirds of the wells are located, have been subsequently reassigned to supergroups on the basis of thickness distributions (Wetmore, 1998; Wetmore et al., 1997).

Complex controls by the basalt/sediment stratigraphy on the

distribution of waste plumes have been identified near injection wells and waste ponds at the INEEL. Packer tests indicate stratigraphic control of an injected tritium plume in basalt flows of contrasting thickness at the Idaho Chemical Processing Plant (Morin et al., 1993; Frederick and Johnson, 1996). The formation of perched groundwater zones at the Test Reactor Area is controlled by the distribution of basalt and thick sediment layers beneath waste ponds (Cecil et al., 1991). The distribution of basalt shields and inferred dikes associated with a volcanic rift zone may control an injected plume of trichloroethylene that is perpendicular to regional groundwater flow directions at Test Area North (Hughes et al., 1997a).

FIELD TRIP GUIDE

Many of the stops in this field trip guide can be enhanced by extended visits and side trips. Unpaved roads are generally adequate throughout the early summer to late fall, but often impossible to travel during the winter and early spring. The first day of the field trip provides an overview of basaltic shield volcanism at Hells Half Acre lava field (Stops 1 and 3), phreatomagmatic volcanism at Menan Buttes along the Snake River (Stop 2), and the relation of the ESRP to the Basin-and-Range province. The second day focuses on mafic volcanism on the axial volcanic zone of the ESRP (Stops 5-9), and surficial processes and hydrogeology on and around the INEEL (Stop 4). Stops on day 2 emphasize lava flow emplacement, basaltic shield growth, and rift systems represented at several locations: Table Legs Butte volcano (Stop 5), the Cerro Grande lava field (Stop 6), and North Robbers spatter cone and lava field (Stop 7). Additional topics on the axial volcanic zone include silicic domes (Big Southern, Middle and East buttes) and Cedar Butte Volcano, a compositionally evolved eruptive center (McCurry et al., this volume). Stop 8 on the second day is at Craters of the Moon lava field, a polygenetic and compositionally evolved center with numerous locations to observe mafic eruptive processes and features of lava flow emplacement along the northern end of the Great Rift. The final stop on the second day is at Box Canyon (Stop 9) and illustrates structural manifestations of basaltic magmatism and glacial cataclysmic flooding. The first half of the third day emphasizes Holocene eruptive and non-eruptive fissure systems at Kings Bowl (Stop 10) and the Wapi lava field, both of which lie near the southern end of the Great Rift. The last part of day three includes Split Butte (Stop 11), a phreatomagmatic tuff ring formation west of the Wapi field, and the Massacre Volcanic Complex, a sequence of basaltic tuffs and lava flows representing several phreatomagmatic vents along the Snake River.

Day One (1/2 day)

Stop 1. Hells Half Acre - part 1 (Dick Smith and Scott Hughes)

Drive northeast on freeway I-15 from Pocatello toward Idaho Falls (Fig. 1); check odometer at the intersection of I-86 with I-15. Drive past the town of Blackfoot (~20 miles), cross the Snake River, and continue for approximately 8 miles past milepost 101. Stop 1 (Fig. 11) is the freeway rest area constructed on the Hells Half Acre lava field which has a radiocarbon age of ~5.2 ka (Kuntz et al., 1986b). Paved trails, one on either side of the freeway, allow easy access to the highly irregular surface typical of all

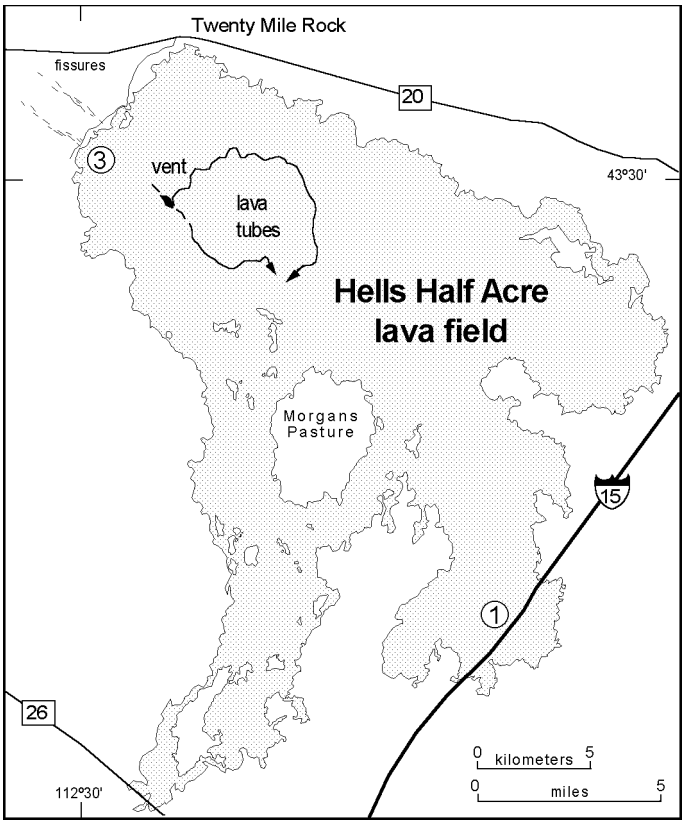

Figure 11. Map of the Hells Half Acre basaltic lava field with Stops 1 and 3 shown in circled numbers. The lava field exemplifies monogenetic Holocene shield eruptions and inflationary lava flow emplacement on the eastern Snake River Plain. Arrows denote path of lava tube feeders.

ESRP lavas which is most readily observed in Holocene examples that are not covered by an eolian blanket. ESRP basalt flows were usually emplaced as tube-fed pahoehoe lavas characterized by numerous collapse depressions (Greeley, 1982). These flows had relatively low viscosity, low width-to-length and low thickness-to-width ratios, and were emplaced as coalescing lobes fed from a central molten interior. Flow lobes were relatively thin and volatile-rich as they emerged from the vent and became thicker and degassed with time and distance from the vent. Most ESRP flows develop small (up to several meters) gas cavities immediately upon eruption forming shelly pahoehoe, and layers of solid basalt on the upper and lower surfaces that is subject to breakage, rafting and formation of brecciated zones. Many flows exhibit a stream-fed component confined by either remnant walls of collapsed tubes or self-constructed levees of chilled basalt.

Pahoehoe lavas normally have numerous squeeze-out areas where molten lava extrudes through cracks in the surface, thus leading to an irregular surface with up to several meters of relief. At the flow front, pahoehoe lobes grow from initial breakouts by either (1) pushing the lobe upward and away from a slow-moving lobe front, or (2) forward expansion as the crust rolls under a fast-moving lobe front (Keszthelyi and Denlinger, 1996). Thin sheet pahoehoe flows, which are not well-represented on the ESRP, have individual lobes typically less than a meter to several meters across. Sheet flows such as those in Hawai'i (Hon et al., 1994) also have an initial thickness of a few tens of centimeters, but the

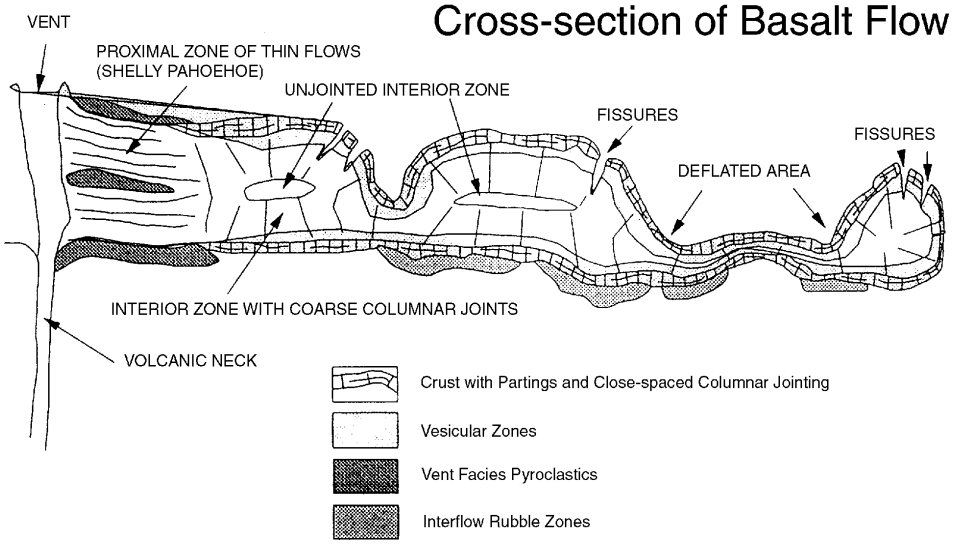

Figure 12. Schematic cross-section of an eastern Snake River Plain basalt flow. The diagram illustrates the inflation-deflation style of pahoehoe lava emplacement typical of ESRP flows, and the irregular surfaces developed during flow and cooling. Flow fronts are typically greater than 5 m thick and the inflated pods range from a few meters to over 100 m across. Adapted from an original unpublished drawing by Richard P. Smith; redrawn version provided by Allan H. Wylie, Lockheed-Martin Idaho Technologies, Inc.

thickness increases dramatically to several meters as magma pushes from within, inflating and lifting the surface.

The morphology of ESRP Holocene lava flows, such as those of Hells Half Acre, indicates that medial to distal parts of flows experienced similar inflationary emplacement styles, but at a much larger scale than that which is typical of Hawaiian pahoehoe lavas. A typical ESRP lava flow facies cross-section (Fig. 12) indicates significant variation in thickness due to collapse. Flow fronts can be as thick as several meters and pahoehoe "toes" several tens of meters across; flow lobes 5-8 m high and ~100 m wide are common. As magma breaks out from an expanding lobe, dramatic deflation results in a basin-like sag of the interior and deep tension fractures (3-5 m deep) along the periphery of the lobe. The collapse increases the irregularity of the flow surface and the number of fractures.

Stop 2. Menan Volcanic Complex (Bill Hackett)

Drive north on I-15 freeway and take Exit 119 at Idaho Falls, continuing northeast on Highway 20. Turn west on Highway 80 about 8 miles south of Rexburg — reset odometer — and travel west towards Annis and Menan. Drive through the town of Annis and at mile 3.6 bear right onto a narrow paved road along the northeast edge of Little Buttes (Fig. 13). At mile 4.1, turn left into quarry for Stop 2A. The Menan Buttes are known to many geologists because they have been used in topographic map exercises of popular introductory laboratory manuals. They are outstanding morphological examples of tuff cones (see Hackett and Morgan, 1988 for detailed discussions).

A few miles south of the Menan Buttes are the remnants of two tuff rings, the North and South Little Buttes, which are much smaller and have lower slope angles than the two tuff rings. The deposits are strongly cyclic and contain abundant accidental quartzite pebbles derived from the underlying permeable alluvium. The tuff rings are dominated by two types of bed sets: black, planar-bedded, coarse scoriaceous lapilli tuff bed sets (mostly fall, with minor surge deposits) were formed during relatively "dry vent" violent strombolian eruptions driven by rapid vesiculation. Intercalated bed sets of tan, cross-stratified, fine palagonite tuffs (fall and surge deposits) were formed during relatively "wet

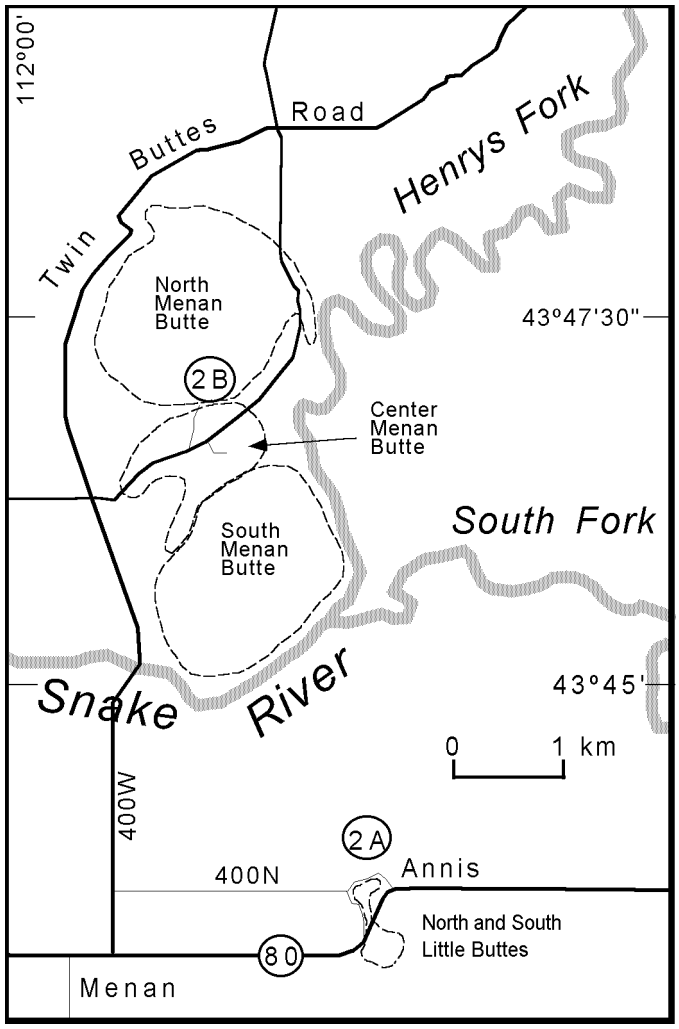

Figure 13. Index map of the Menan Buttes phreatomagmatic tuff cones with field trip stops shown in circled numbers (2A, 2B). The Menan Volcanic Complex includes North, Center and South Menan Buttes (2B), as well as North and South Little Buttes (2A). Compare to Fig. 9.

vent" surtseyan eruptions driven by phreatomagmatic processes.

From Little North Butte quarry — reset odometer — head west on road 400N. Turn left (north) at mile 1.9 on road 400W and drive toward the Snake River. Cross the bridge (mile 3.7) and at mile 5.1 turn right (east) onto the unmarked, improved gravel road that heads northeast, between North and South Menan Buttes. At mile 6.0 turn left onto an unmarked road towards the south flank of North Menan Butte and park at mile 6.2 for Stop 2B. Walk up the gully to observe excellent tuff exposures and, if time permits, reach the southern crater rim where densely palagonitized tuffs and large ballistic blocks are exposed.

The Menan Buttes tuff cones are the largest features of the Menan volcanic complex, with reconstructed volumes of 0.7 (North) and 0.3 (South) km^3. Dense basalt volume equivalents are 0.4 and 0.2 km^3, respectively. They are among the largest terrestrial tuff cones, with volumes comparable to those of Diamond Head, Oahu, and Surtsey, Iceland. Deposits of the North and South Menan Buttes tuff cones are monotonous, massive to thin-bedded, tan, lithified palagonite lapilli tuffs with minor xenoliths of dense basalt and rounded quartzite pebbles. At this stop observe weakly convoluted, thin-bedded tuff, and bed forms that are nearly obliterated by palagonitization.

Stop 3. Hells Half Acre - part 2 (Dick Smith and Bill Hackett)

Drive southwest on Highway 20 back to Idaho Falls, take I-15 southbound from Exit 119 to Exit 118 — reset odometer at the exit, and continue on route 20 west-northwest for 20 miles to Twenty Mile Rock. A bend in the road at this point allows traffic to skirt around the Hells Half Acre lava field visible to the south. At mile 20.2, turn left (southwest) on Twenty Mile Rock Road (the first unpaved road after the curve), remain on the road closest to the lava field where it forks (about one mile), and continue to mile 22.8, 2.6 miles from the highway, to Stop 3 (Fig. 11) along the margin of the lava field. The vent area of the Hells Half Acre lava field is located in the northwest part of the lava field, ~4 km southeast of this stop. It is a northwest-elongated crater containing several deep collapse pits. A northwest trending eruptive fissure, located just south of the crater (Kuntz et al., 1994) and short sections of eruptive fissures located between the crater and this field trip stop suggest that the feeder system for the lava field is a northwest-trending dike. This is consistent with the observation that ESRP volcanic rift zones trend northwestward, almost perpendicular to the trend of the plain itself (Kuntz et al., 1992), and to the interpretation that the orientation of dikes, as well as non-eruptive fissures and vent alignment, are controlled by the same (northeast-trending extension) stress field that produces Basin-and-Range faulting adjacent to the ESRP (Hackett and Smith, 1992; Smith et al., 1996).

At this stop, two sets of non-eruptive fissures, flanking the eruptive fissure (feeder dike), extend northwestwardly from beneath the edge of the Hells Half Acre volcanic field (Kuntz et al., 1994). A several-meter-thick eolian blanket underlies the lava field obscuring much of the fissuring, but in several places the loess and sand has collapsed into the fissures and/or has been eroded into the fissures by percolating or flowing water. The fissure sets, separated by a distance of about 1.5 km, were caused by a zone of extensional stress above the non-eruptive part of the dike (Fig. 7). These are typical surface deformational features associated with shallow dike intrusion in volcanic rift zones (Pollard et al., 1983; Rubin and Pollard, 1988; Rubin, 1992; Smith et al., 1996). Fissure widths are generally less than 1 meter, and the fissure walls are very irregular because pre-existing columnar jointing in the lava flows controlled the near-surface fissure shape. Parallel sets of non-eruptive fissures (well-known in Iceland, Hawai'i and Galapagos) are also observed along the Great Rift between Kings Bowl lava field and the Craters of the Moon lava field (Kuntz et al., 1988) and in the Arco volcanic rift zone (Hackett and Smith, 1994). In addition, a small graben (~300 meters across, ~10 meters of vertical displacement, and several km long) occurs in the northern part of the Arco volcanic rift zone. We will visit this graben on day 2 of the field trip (Stop 9). This is the last stop of the first day.

Day Two

Stop 4. Axial Volcanic Zone, INEEL hydrogeology, and ESRP environmental geology overview (Dick Smith, Bill Hackett, Steve Anderson)

Drive on I-15 (northeast from Pocatello or southwest from Idaho Falls) to Blackfoot Exit 93, turn northwest onto Highway 26, and reset the odometer at the stoplight immediately west of the I-15 underpass. Continue driving past the industrial/commercial complex and, at mile 4.0, begin watching for outcrops and roadcuts through fresh lava flows. While driving through this area, note sheet lavas, inflated lobes and pressure ridges of Hells Half Acre basalt near the southernmost limit of the lava field. Proceed to mile 17, near a topographic high point on the northeast side of the highway which is the eruptive center for the ~165 ka Taber Butte lava field (Kuntz et al., 1994). Carefully park on the shoulder and walk up the ridge to Stop 4 for a panoramic view looking northwest toward the axial volcanic zone and the INEEL (Fig. 14). At this point there will be an overview discussion of the axial volcanic zone, silicic domes (Big Southern, Middle, and East buttes), hydrogeology of the INEEL, and environmental issues on the ESRP.

Pleistocene rhyolite domes and at least one complex eruptive center occur along the axial volcanic zone on the ESRP (Figs. 15, 16). Big Southern Butte is the largest ESRP rhyolite dome formed of two coalesced endogenous lobes (Spear and King, 1982) with K-Ar ages of 294 ± 15 and 309 ± 10 ka (Kuntz et al., 1994). An uplifted, north-dipping block of basalts, ferrolatites and sedimentary interbeds occurs on its north flank (Fishel, 1993). Chemically evolved ferrolatites imply the existence of a complex volcanic center in the vicinity. A possible source of these lavas is the Cedar Butte eruptive center (Spear, 1979; Hayden, 1992), ~8 km east of Big Southern Butte. Cedar Butte is a complex assemblage of landforms and chemically evolved lavas with a radiometric age of ~400 ka (Kuntz et al., 1994), mostly intermediate in composition but including a rhyolite lava flow. A topographic escarpment southeast of the summit may be the result of uplift associated with late-stage silicic-magma intrusion beneath the complex, or the draping of mafic lava flows over a steep-sided silicic flow (see McCurry et al., this volume, for a more detailed discussion of petrogenesis). Middle Butte is a stack of about twenty basalt lava flows, apparently uplifted in pistonlike fashion by a buried

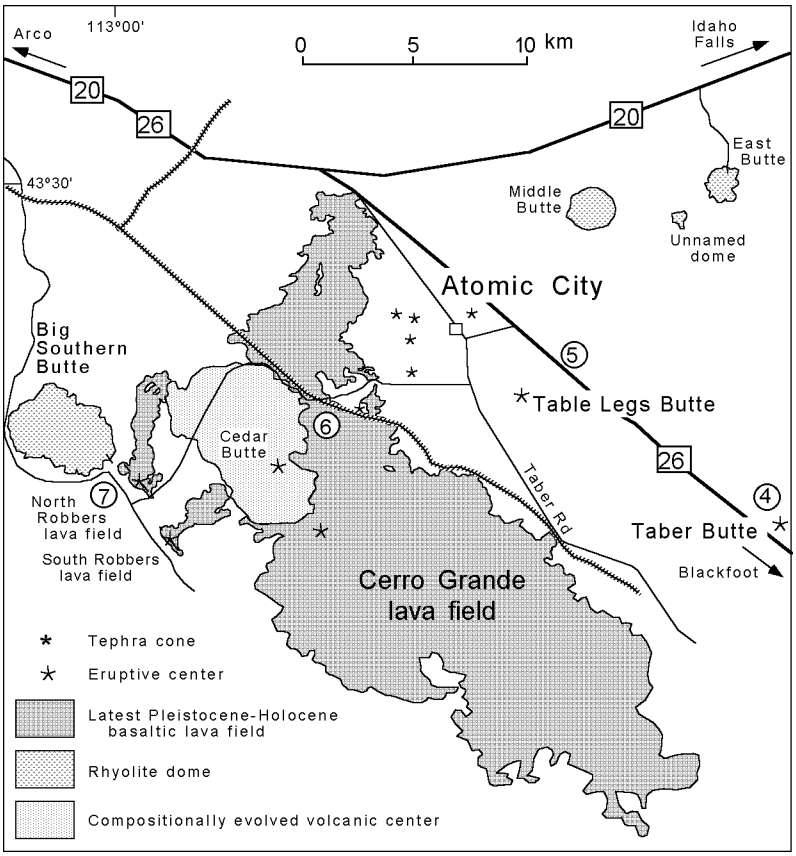

Figure 14. Detailed index map of the Cerro Grande lava field, North and South Robbers lava fields, and other features along the axial volcanic zone, adapted from Kuntz et al. (1992), aerial photographs and field investigations. Field trip stops are shown in circled numbers. See text for explanation and road guide to Stops 4-7.

silicic cryptodome of unknown age. East Butte is a ~1.4 Ma (Armstrong et al., 1975) endogenous rhyolitic dome, in places containing centimeter-sized clots and blocks of mafic material (Kuntz and Dalrymple, 1979). A small unnamed rhyolite dome dated at ~0.6 Ma (Kuntz et al., 1994) lies between Middle and East buttes.

Recent range fires on and near the INEEL provide real-time observations of eolian sediment redistribution processes on the ESRP. Since early 1994, nine range fires burned over 60,000 acres (95 square miles) of sage and grasslands. Ensuing dust storms whipped up by prevailing winds caused highway closures and shutdowns of work at some INEEL facilities. Measurements of soil erosion using erosion bridges (Olsen, 1996) and estimates of removed material using height of charred stubble above deflated ground surface indicate that millions to 10's of millions of cubic meters of fine-grained sediments have been mobilized. Very rapid development of new landforms and modification of existing landforms occurred. Within a few days of a 17,000 acre fire in the western part of INEEL in 1994, a discontinuous "dune", 20 km long, 1 m high, and several m wide, formed along the eastern (downwind) edge of the fire scar. A 2-m wide fissure along the east edge of the scar was filled with sediment after the first wind storm.

In the eastern INEEL a 19,000-acre fire in 1996 burned an area that contained a prominent lineament, called the Principal Lineament, which was itself formed by eolian modification of a prehistoric fire scar (Morin-Jansen, 1987). Unique patterns of vegetation, including luxuriant stands of basin wild rye and tall sage, developed on the Principal Lineament because of the relatively coarser sediment with better water holding capacity there. The presence of abundant grasses with good soil-stabilization root systems may preserve the Principal Lineament through this new cycle of burning. Aerial and surface monitoring of the new fire scar as it is revegetated over ensuing years will keep track of the fate of the Principal Lineament and the potential development of new lineaments.

The size, shape, and age variations of numerous historic and prehistoric fire scars on the ESRP, observable on aerial photographs and Landsat images, suggest a continuing process of eolian redistribution of loess following range fires. Implications of the process include: (1) Range fires tend to have the same shapes and sizes in various parts of the plain, reflecting similar prevailing wind directions and fire dynamics. (2) Lineaments are formed and destroyed repeatedly by range-fire and eolian processes. (3) Over the long term, sediment is continually on the move in a down-wind direction. (4) A sorting of the upper few centimeters to decimeters of soil may occur, with fine material being moved farther downwind and coarser material lagging behind. (5) Open fissures in volcanic rift zones may have been filled many times by eolian deposition following range fires and subsequently opened by percolation and piping of water into deeper fracture zones and rubble zones in the volcanic sequence.

Figure 15. East Butte rhyolite dome (view from the southwest), one of several Pleistocene silicic volcanic domes on the eastern Snake River Plain axial volcanic zone (see Fig. 14).

Stop 5. Table Legs Butte (Scott Hughes)

Continue driving northwest on Highway 26 to a shallow roadcut at mile 24.2 (near milepost 280) for Stop 5 (Fig. 14), where the ESRP can be viewed from the elevated axial volcanic zone. Pleistocene to Holocene basaltic volcanism across the ESRP produced hundreds of small shield volcanoes that have low-angle slopes, cover tens to hundreds of square kilometers, and were built by overlapping pahoehoe lava flows (Hackett and Morgan, 1988). Table Legs Butte, conveniently located outside the boundary of the INEEL and approximately 2.5 miles southeast of Atomic

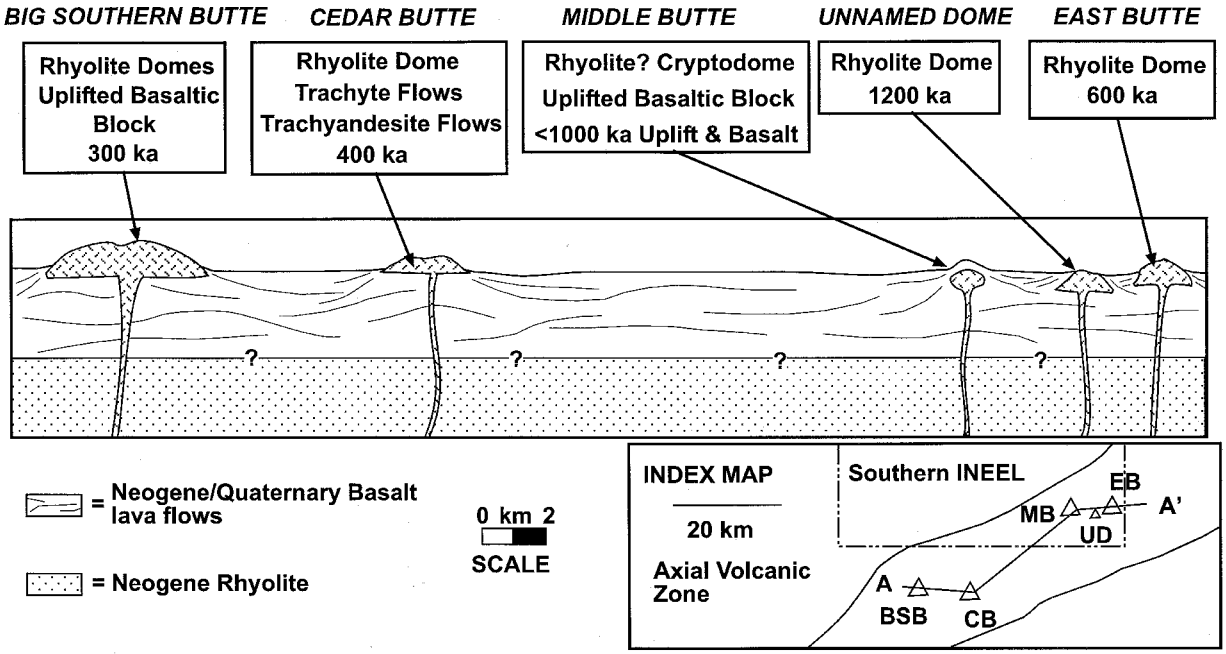

Figure 16. Schematic cross section along the axial volcanic zone of the ESRP, showing the ages, rock types and known or inferred lithostratigraphic relations of Pleistocene silicic volcanic domes (adapted from p. 146, Link and Phoenix, 1996; and Hackett and Smith, 1992).

City, is one of several basaltic shields on the axial volcanic zone not associated with any of the major volcanic rift zones (e.g. Kuntz et al., 1992). Spatter ramparts surround a prominent summit region flanked by low-angle slopes on the shield. Lavas from this shield are probably 200-400 ka based on geomorphic and stratigraphic relations with other shields (Kuntz et al., 1994); hence most flow surfaces have substantial chaparral vegetation growing in late Pleistocene and Holocene eolian soil.

In roadcuts near milepost 280, observe cyclic diktytaxitic texture and vesiculation described above (Fig. 17). Table Legs basalt in this roadcut contains abundant, up to 40%, phenocrysts of subhedral-to-euhedral plagioclase laths ranging from 0.7 to 1.5 cm in length and less abundant phenocrysts of 1-2 mm olivine. Cyclic layering in phenocryst size and abundance occurs in strongly diktytaxitic shelly pahoehoe, and represents a feature that can be observed in lavas from several basaltic shields on the ESRP. Textures range from fine-grained nearly aphyric to coarse porphyritic with plagioclase laths up to 1 cm comprising over 20 percent. In some cases, aphyric lava has filled tension fractures developed in plagioclase-phyric lava. Alternating crystal-rich and crystal-poor layers were possibly derived by crystal-liquid segregation during compression and decompression processes within molten cavities that allowed residual liquid to drain out of a crystal network. Crystals are usually intact and either randomly oriented or clustered into star-shaped patterns.

Figure 17. Cyclic layering of diktytaxitic texture in basalt from Table Legs Butte illustrating relative aphyric and coarsely crystalline horizons (Stop 5) possibly caused by liquid segregation from the crystalline skeleton and chilling of individual pulses of magma. The effect is attributed to cyclic increase and decrease of magma supply within tube-fed lava flows as cooling crust is inflated and deflated during lava flow emplacement.

From this point, one can see that Table Legs Butte is a complex, multiple vent shield volcano although evolved compositions similar to those found in Cedar Butte and Craters of the Moon complex eruptive centers have not been documented. Aerial photographs indicate that the Table Legs eruptive center is fairly small, approximately 98 km^2, with a ridge of at least 4 eruptive vents on the east flank ~1-2 km from the main vent. These are interpreted as primary vents, the surface expression of dikes along a local rift system, that possibly stopped erupting as volcanism became more concentrated toward the summit region. Smaller vent-like features, mostly squeeze-ups and rootless vents occur on the west and north flanks, some of which are aligned due to breakout along tube-fed flows from the main vent.

Stop 6. Cerro Grande lava flow (Scott Hughes and Dick Smith)

Drive northwest on Highway 26 to mile 26.6, turn west at Magee's pub on Midway Road, proceed to mile 28.0 and turn south on Taber Road at the south end of Atomic City. Drive to mile 29.3 and turn west onto improved unpaved road; continue to

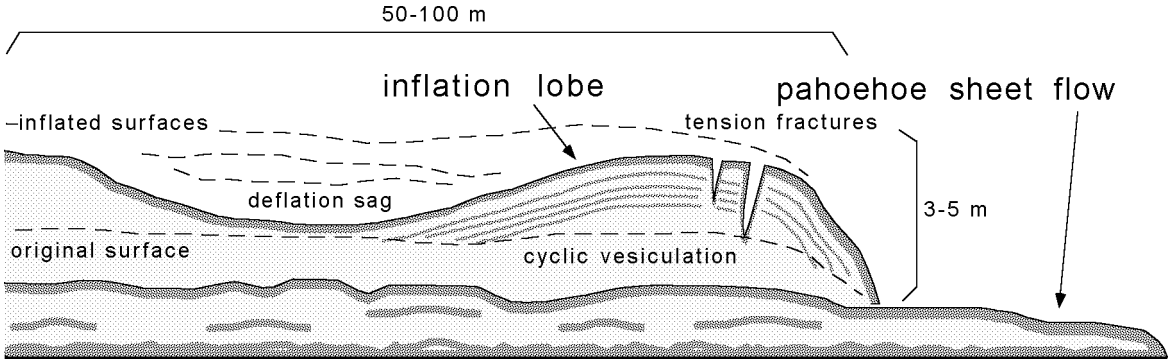

Figure 18. Schematic diagram of thick inflationary pahoehoe lobe over thinner sheet-like pahoehoe flow observed in the Cerro Grande basalt at Stop 6. Cyclic vesiculation, tension fractures, and sagging are related to repeated pressure fluctuations within the lobe while the solid crust becomes thicker with cooling.

mile 33.2 at a railroad crossing near the margin of the Cerro Grande lava flow for Stop 6 (Fig. 14) and park on the west side of the tracks. This will be a good opportunity to observe the flow margin of Cerro Grande lava, dated by radiocarbon at 13,380 ± 350 (Kuntz et al., 1986b), and the effects of inflationary emplacement of pahoehoe lavas typical of ESRP basalts. The flow margin comprises two parts: a thin outflow "sheet" pahoehoe and an overlying thicker flow made of large inflationary pahoehoe lobes (Fig. 18).

Vesicles and mineral textures reflect variable pressures inside inflating and deflating lava lobes. Layers of vesicles occur in cycles, often as 1-2 cm layers of intensely vesiculated lava separated by 10-20 cm of more massive lava (Fig. 19) representing repeated pressure increase during lobe inflation followed by decompression and volatile exsolution. Thickness of the crust increased with each cycle. The vesicle layers are curved and concentric with lobe surfaces rather than horizontally oriented, due to gravitational rise of bubbles, such as those noted for vesicle layers within Columbia River basalt flows (Manga, 1995). This suggests that molten lava within each lobe experienced cyclic velocity changes as magma repeatedly backed up during marginal cooling then broke out when internal pressure rose above the tensile strength of the crust. Similar processes are noted for sheet flows in Hawaii (Hon et al., 1994)

Figure 19. Cyclic vesiculation in Cerro Grande lava observed at Stop 6.

Climb up the 5-8 m lobe on the northeast side of the tracks where deflationary sagging has resulted in deep tension gashes along the periphery. From this point, one can observe cyclic vesicle layers in the fracture walls related to repeated decompression of the lobe interior as the crust thickened downward. The flow surfaces on the top and flank of the lobe are ropy pahoehoe, typical of the thinner sheet flow on the lower level, that were originally close to horizontal. This observation attests to the significant amount of inflation necessary to produce several meters of uplift due to internal magmatic pressure or gas pressure caused by volatile exsolution.

Stop 7. North Robbers vent (Dick Smith and Scott Hughes)

Drive west from the railroad crossing on the improved unpaved road for ~2.8 mi and note the intersection with a southbound unimproved dirt road. This road will provide access to Cedar Butte volcano (McCurry et al., this volume), a complex intermediate-silicic eruptive center on the axial volcanic zone. Continue west on the improved unpaved road to mile 39.8, and turn right onto a service road. Drive as far as possible, approximately 0.2 mi, to Stop 7 which is located at the vent for the North Robbers lava field (Fig. 14). This is one of the three smallest lava fields (along with South Robbers and Kings Bowl) in the late Pleistocene and Holocene episode of ESRP volcanism. The fissure zone for North Robbers is 2.9 km, and separated into a 1-km-long northern segment, which has both eruptive and non-eruptive components, and a 1.2-km-long southern eruptive segment (Kuntz et al., 1992). The non-eruptive part of the northern segment extends northwest into the Big Southern Butte rhyolite dome. The southern segment is offset from the northern segment and is the primary eruptive fissure system for the North Robbers lava.

Hike up to the summit region which is constructed by a spatter rampart at the vent. This is a good vantage point to observe fairly uncomplicated eruptive features associated with ESRP basalts. On the north side of the cone, the flow extends north-northeast from the vent area through a lava channel. Walk around to the southeast side to observe the eruptive fissure system oriented northwest-southeast along the Arco volcanic rift zone from which a relatively short lobe of fissure-fed lava flowed northeast. Return to the vehicles and proceed west on the improved road, go past the turnoff to Crossroad Well at mile 43.4, and continue north-

ward around Big Southern Butte to mile 47.1, which is a junction of Frenchman Cabin and the road access to a landing strip on the northwest side of the mountain. Proceed north, around the southwest end of the landing strip, and stay on the improved road for ~12 mi to Highway 20/26. Turn west and drive to Arco.

Stop 8. Craters of the Moon and the Great Rift (Scott Hughes, Bill Hackett and Dick Smith)

Drive southwest from Arco on Highway 20/26 (~18 mi) to Craters of the Moon National Monument and park briefly at the visitor's center for Stop 8A. Covering about 1,600 km^2 with about 30 km^3 of basaltic and compositionally evolved lava flows, Craters of the Moon is the largest and most complex of the late Pleistocene and Holocene ESRP basaltic lava fields. Eight eruptive periods occurred from 15,000 to 2,100 years ago with quiescent intervals as long as 3000 years (Kuntz, 1989; Kuntz et al., 1982, 1988, 1992). Eruptive vents are aligned along the northern part of the Great Rift, northwest of the Kings Bowl and Wapi lava fields in the same rift system. Lava flows differ chemically and petrologically from typical SRP olivine tholeiites (Fig. 8). Craters of the Moon lavas have olivine tholeiitic parent magmas, but they are fractionated to ferrolatites and exhibit chemical characteristics of crustal contamination. Relative to typical ESRP basalts, their compositions exhibit higher Ti, Fe, Na, K, P and lower Mg, Ca.

The Craters of the Moon lava field has nearly every type of feature associated with basaltic systems. Within a few hours time one can observe pahoehoe, a'a, and block lava flows, plus bombs, blocks, scoria and glassy basalt. Spatter cones and cinder cones with widely ranging tephra size fractions reflect variable viscosity and eruptive mechanisms. Vent alignments along fissures and multiple eruptive phases within the larger craters are evident. Lava flows exhibit squeeze-ups, pressure ridges, lava tubes, levees, hornitos, driblet cones and spires, lava stalactites, tumuli, kipukas, extension cracks, scarps, rafted blocks, and tree molds. Please note that off-trail hiking is allowed anywhere in Craters of the Moon National Monument except for the spatter cones area and the North Crater Flow. Absolutely NO sampling is allowed anywhere in the monument.

After a brief stop in the visitor center follow the park road (Fig. 20) across North Crater Flow (note large rafted blocks of agglutinated tephra), around North Crater and Paisley Cone, between Big Craters and Inferno Cone to the Spatter Cones parking area. This is Stop 8B, where three small spatter cones, one with perpetual snow and ice in the crater, are aligned with Big Craters cinder cone complex along a fissure. Walk ~50 m over to the closest spatter cone to observe the plastically-deformed agglutinate in a high angle of repose. Inside the cone observe drainback features and the highest level of lava rise during the eruptive phase. This feature is evidence, as observed in many Hawaiian spatter ramparts, of oscillating magma input that would contribute to cyclic changes in hydraulic head of lavas and inflation of pahoehoe lobes.

Hike ~100 m northwest along the trail up to the rim of Big Crater and note the tephra stratification sequence on the opposite wall and nested eruptive pits in the floor. At least three eruptive phases are evident from the rim at this location; more can be seen

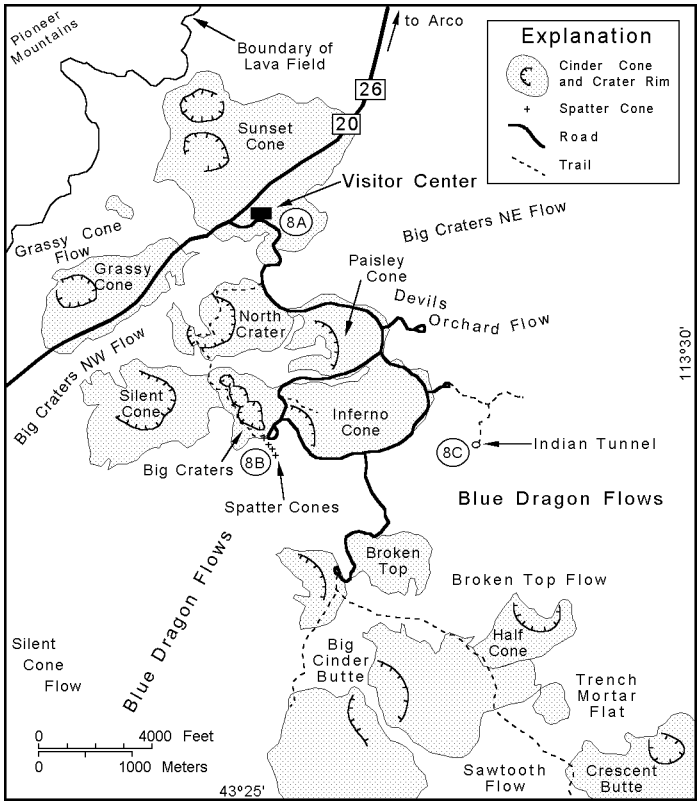

Figure 20. Index map of the Craters of the Moon National Monument area (adapted from Kuntz, 1989) showing tephra cones and general locations of major lava flows. Field trip Stops 8A-8C are only a few of the numerous places in the monument where fresh volcanic features can be observed.

on a brief walk around the rim. Facing south, observe the Blue Dragon lava flows, the youngest in the lava field (Kuntz et al., 1988), which exhibit the characteristic smooth pahoehoe surface sheen punctuated by rough zones of a'a lava.

Continue southeast on the park road (Fig. 20) between the Inferno Cone and Blue Dragon lavas, then to lava tubes in the Blue Dragon flows (Stop 8C) and prepare for hiking in cool dark conditions. Follow the marked paved trail eastward ~0.5 km to Indian Tunnel, a lava tube with several collapsed roof sections that allow hiking without artificial illumination. While hiking through this cave (~100 m) observe the walls and floor and note various lava levels, stalactites and drainouts from alcoves that occurred when the tube was emptied. In particular, notice the floor in places where ceiling blocks have not obscured the original texture of the flow surface. The cooling rate was obviously much lower inside the tube so the floor is not glassy-smooth like the outside surfaces. Instead, a cm-scale roughness is evident that was likely caused by stretching and buckling while the surface cooled much slower than the flow surface outside the tube. Other caves may be visited before continuing on to the next stop.

Leave the caves area and continue around the northeast side of Inferno Cone and east side of Paisley Cone to Devils Orchard. At this point observe the rough block and a'a flows that formed from higher-viscosity latite lava. This flow probably erupted from

North Crater (Kuntz, 1989); it has steep 5-m flow fronts and 20-m-high rafted blocks of bedded cinders derived from the cone. Leave the monument through the front entrance, drive northeast on Highway 20/26 back to Arco, and reset the odometer downtown at the intersection with U.S. Highway 93.

Stop 9. Box Canyon and glacial outburst flooding (Dick Smith and Bill Hackett)

Drive southeast from Arco on Highway 20/26 to mile 1.3, and turn right at an intersection of two improved unpaved roads, one bearing south and the other bearing west. Drive south and southeast to an intersection at mile 2.4, continue on the south (right) branch to mile 4.6, across the bridge over Big Lost River, to an intersection where the "main" road (left branch) continues southeast. Follow this road to mile 5.9, then turn northeast (left) and go to mile 6.7 where the road takes several bends near the edge of Big Lost River and drops down in elevation for Stop 9A (Fig. 21). Upstream (northwest) from this point, the river flows within and parallel to the Arco volcanic rift zone (Fig. 10). Downstream, it flows northeast, then back southeast along the rift trend cutting into ESRP basalts forming Box Canyon.

This stop is on the southwest margin of the Box Canyon graben (Fig. 22), a linear northwest-southeast topographic depression that controls the Big Lost River and marks the northern extent of dike-induced structures in the Arco volcanic rift zone. From this point and southeastward to Big Southern Butte, Arco volcanic rift zone surface deformation and vents (Smith et al., 1989, 1996; Hackett and Smith, 1992) are typical of those observed in volcanic rift zones in Iceland and Hawai'i (Pollard et al., 1983; Rubin and Pollard, 1988; Rubin, 1992). Fissures, fissure swarms, small normal faults, graben, eruptive fissures, and monogenetic shield volcanoes are abundant in this zone. From this point northwestward to the town of Arco, the origin of structures is ambiguous and transitional to the Lost River fault, which is offset relative to Box Canyon and well developed north of Arco. The identification of late Quaternary fault scarps on the Lost River fault is clear and unequivocal from Arco to the north, but terraces along the Big Lost River and Holocene incision and deposition along a small drainage that joins the Big Lost River just south of Arco obscure any possible fault scarps and make identification of the fault uncertain (Scott, 1982). Reflection seismic surveys show displacements attributable to the Lost River fault for a distance of about 5 or 6 km south of Arco, but none in the area of the Box Canyon graben. Because of the uncertainty in fault identification, and the distance of possible epicenters of earthquakes to INEEL facilities is sensitive to the position of the southern end of the Lost River fault, several scenarios for the southern termination are used in seismic hazards assessment.

The Box Canyon graben probably represents the cumulative effects of several dike intrusion events into this part of the volcanic rift zone. The tilting of slabs of basalt and the fan-like separation of columnar joint blocks, typical of deformation due to dike intrusion in volcanic rift zones worldwide, is visible here (Fig. 22) in the area where the river cuts into the northeast limb of the graben. Figure 7 illustrates the relationship of volcanic rift zone grabens to dikes in the shallow subsurface.

Drive southeast from Stop 9A ~0.1 mi to a fork, continue on the left branch to a junction at mile 8.5 mi and take the left branch, which is the main road traveled before turning off to Stop 9B. Drive southeast to mile 9.8, take the left fork, continue another 1.0 mi and turn northeast (left) onto a service road for 0.2 mi which leads to a well for Stop 9B at mile 11.0 (Fig. 21). This stop is in the Arco volcanic rift zone southeast of Box Canyon graben where clear evidence exists for a late Pleistocene glacial outburst flood(s) (Rathburn, 1991, 1993). After an overview of glacial flooding, observe the erosional loess scarp and walk around on basalt stripped bare of soil. Erosional features caused by the flooding include cataracts in basaltic terrain, scabland topography, and scouring of

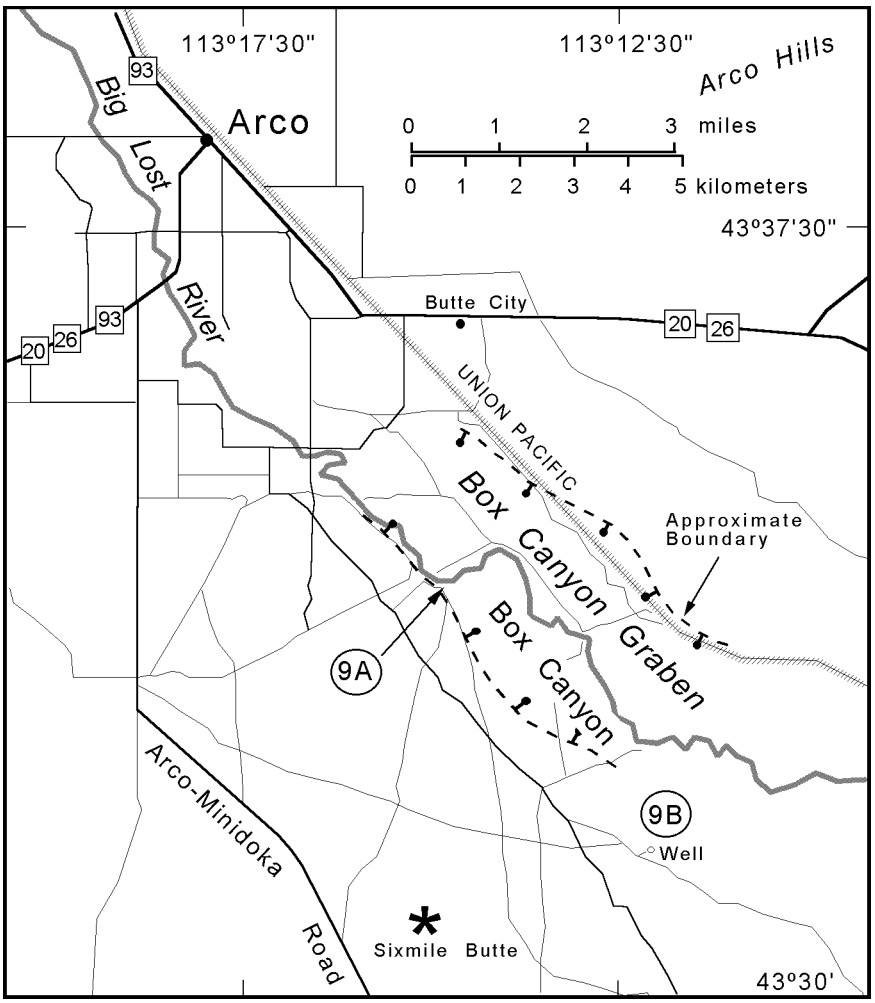

Figure 21. Map of unimproved roads (thin solid lines) south of Arco, Idaho illustrating access to Box Canyon graben. The Big Lost River flows southeast in a direction structurally controlled by the Arco volcanic rift zone (see Fig. 10). Stop 9A allows observation of Box Canyon graben, which follows the same structural trend. Geomorphic features related to catastrophic glacial flooding are observed at Stop 9B.

Figure 22. Box Canyon graben and Big Lost River at Stop 9A, view from the northwest looking downstream where the river cuts into the most recent lava flow.

loess from the basalt lavas, leaving a scarp that marks the edge of the flood. The loess scarp and scoured basalt surface can be recognized on landsat images of the area. Depositional features include boulder bars and ice-rafted erratic boulders. Flood discharge was 60,000 cubic meters per second. The age of flooding was about 20,000 years B.P., near the time when several other glacial outburst flooding episodes occurred in the western U.S., and may mark the beginning of glacial melting after the last glacial maximum (Cerling et al., 1994). This is the last stop for day 2; retrace the route back to Highway 20/26 and proceed to Pocatello. Note: It is possible to make a connection to stops on day 3 using the Arco-Minidoka Road (Fig. 23); however, travel on this adventuresome road often requires four-wheel drive and is not advised during seasonal periods of heavy intermittent rains or snow.

Day Three

Stop 10. Kings Bowl Lava Field (Scott Hughes and Dick Smith)

Drive west from Pocatello on I-86 to Exit 40 at American Falls, take the bypass around the city and continue across the dam that backs up the reservoir. Reset the odometer at the intersection to Lamb Weston immediately past the dam and continue north on route 39 to mile 5.0. Turn west on North Pleasant Valley Road, go to mile 13.5 where a cemetery on the right marks the intersection with Quigley Road and turn north. Proceed north to mile 14.5 and turn west on Schroeder Road which becomes Roth Road farther west. Continue west on Roth Road to mile 16.7, turn north on Winters Road, and drive to a fork at mile 19.4. A sign at this location indicates mileage to Wapi Park (8), Arco-Minidoka Road (16), and Bear Trap Cave (16) (see Fig. 23). Take the left fork, drive past an intersection at mile 22.6, and another intersection at mile 23.4, and stop briefly at mile 25.6 for Stop 10A (Fig. 24). Note: Wapi Park, located at the margin of the Wapi lava field, can be reached by taking the (rugged) road at mile 23.4. It is an excellent place to camp, with no facilities or water, and hike to Pillar Butte, the eruptive center for the lava field.

Walk west toward the margin of the sheet pahoehoe flow that erupted from the Great Rift at the Kings Bowl fissure system. Before reaching the edge of the lava there will be several segments of non-eruptive fissures visible as shallow depressions in the eolian soil. A meager amount of searching will reveal actual fissures in the underlying basalt where the exposure is enhanced due to loss of loose eolian material down the cracks. Some fissures can be traced for several tens of meters, and most are visible in aerial photographs.

Continue on the road another 0.1 mi, take the left fork and drive to the Kings Bowl lava field at mile 26.1 for Stop 10B (Fig. 24). Park in the area once reserved for public visitors on the northeast side of the rift (the visitors center is now abandoned) and walk northwest along the fissure system to gain access to the opposite side. For an extended field trip, Greeley et al. (1977) provide an excellent and much detailed guide to this lava field. There are many places along the rift and on the lava field that are potentially dangerous to hikers and climbers, so be alert when working

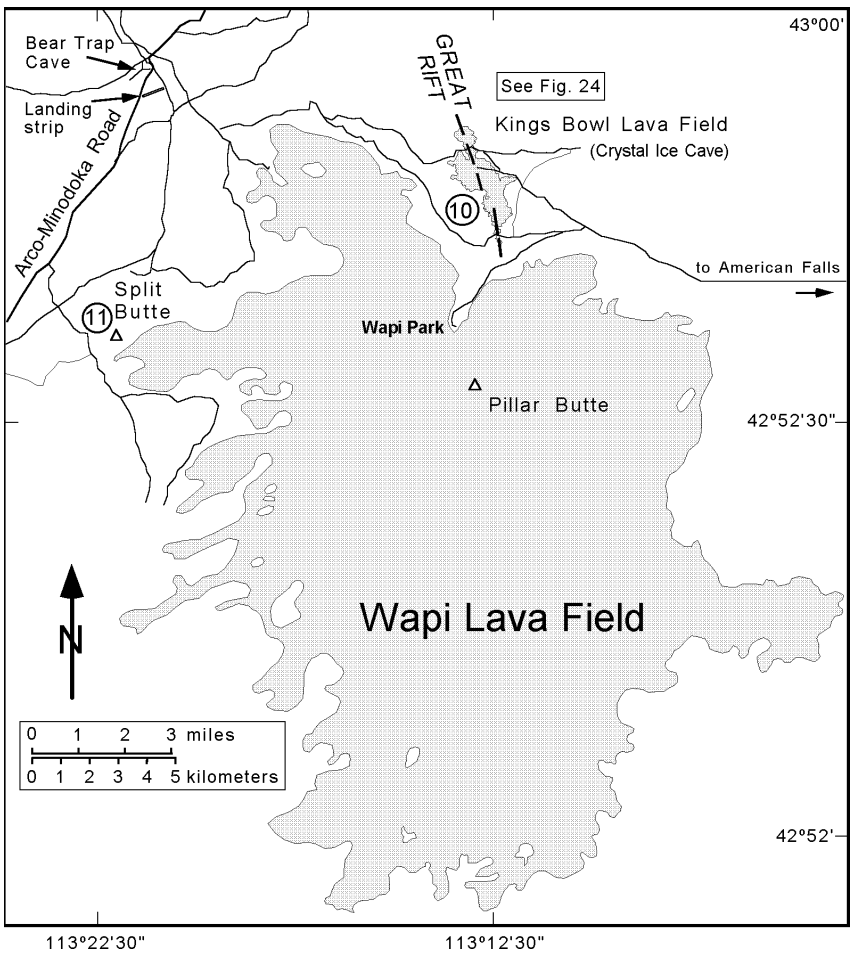

Figure 23. Index map of the Kings Bowl (Stop 10) and Split Butte (Stop 11) areas showing access roads (thin solid lines) and the boundary of the Holocene Wapi lava field.

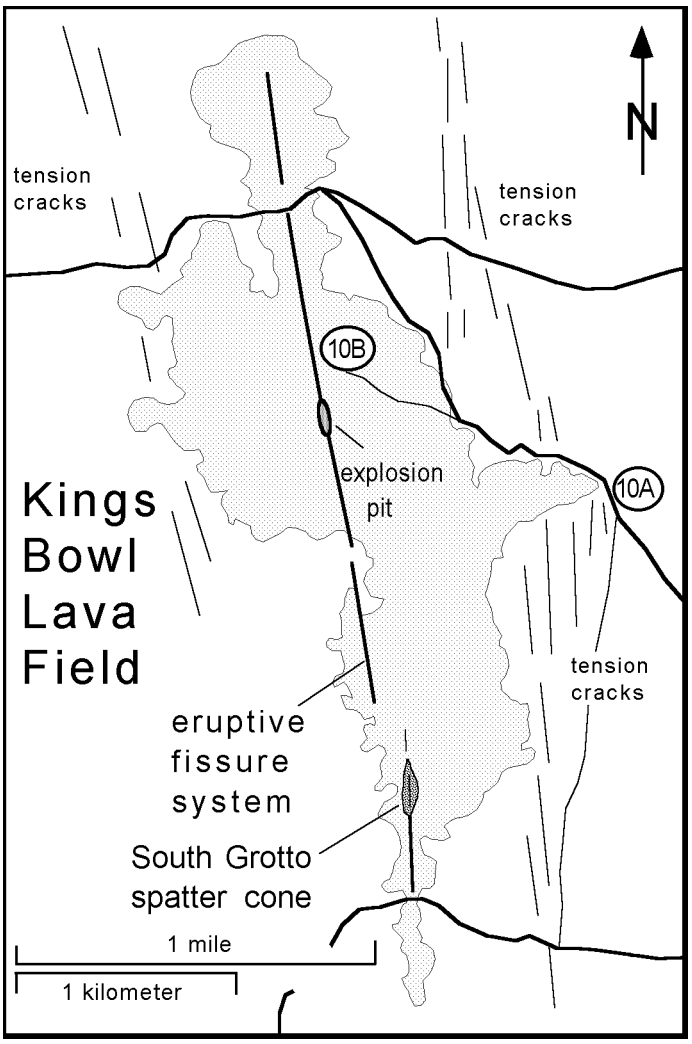

in this area which is a popular attraction to spelunkers. Recent events, including at least one fatal accident, have prompted the U.S. Bureau of Land Management to post signs warning of dangerous cliffs and deep chasms related to the Great Rift and the Kings Bowl eruptive center. However, much can be observed here without resorting to technical climbing into the deeper recesses of the rift system.

Radiocarbon dating of this eruption (Kuntz et al., 1986b) indicates an age of 2,222 ± 100 years B.P., and Kuntz (1992) suggests that the field represents a single burst of activity over a period possibly as short as six hours. Kings Bowl (the phreatic explosion pit) and Crystal Ice Cave (a section of the fissure system) have been visited extensively by the public and received much attention in geologic studies (Greeley et al., 1977; Kuntz et al. 1982, 1992). Fissure-fed lava issued from numerous points along a 6.2-km-long en-echelon fracture system (Fig. 25). Two sets of non-eruptive fractures approximately 1.5 km apart occur on opposite sides of and parallel to the central eruptive fissures (e.g. Stop 10A).

The Kings Bowl lava field (Fig. 26) is the smallest of three eruptive centers, besides Wapi and Craters of the Moon, on the Great Rift, yet it provides an ideal place to observe many features related to an ESRP fissure eruption that culminated in a phreatic

Figure 24. Detailed map of Kings Bowl lava field illustrating eruptive and non-eruptive fissures and associated tension fractures that formed as a result of dike injection (see Fig. 7). Crystal Ice Cave and Kings Bowl have been popular attractions to tourists and adventurers for many years. Kings Bowl is a phreatic pit that was excavated during the culminating eruptive phase of the fissure-fed flow. South Grotto is an elongate spatter rampart deposited along the southern part of the eruptive fissure.

Figure 25. Segment of the fissure system at the Holocene Kings Bowl lava field located along the Great Rift volcanic rift zone on the eastern Snake River Plain.

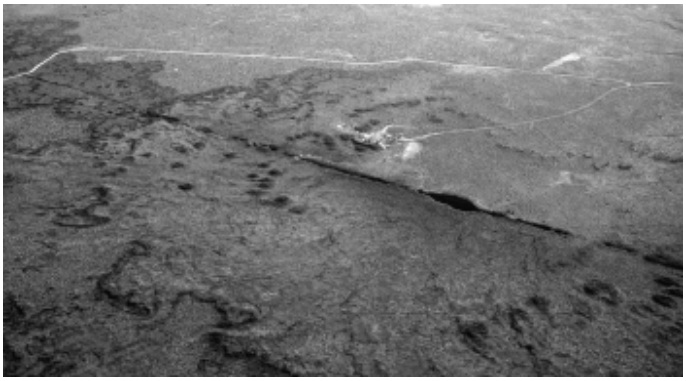

Figure 26. Kings Bowl lava field, viewed looking northeast across the Great Rift and illustrating the prominent eruptive fissure system. Kings Bowl, a phreatic blowout crater, is the elongate gaping part of the fissure just right of center in the photograph. The Crystal Ice Caves parking area lies just northeast of the fissure.

phase. A final explosion occurred in a short segment of the rift following relatively quiet emplacement of a sheet pahoehoe flow along the several km-long eruptive fissure. The explosion ejected blocks of chilled Kings Bowl lava and older flows up to several meters creating a pit that is 85 m long, 30 m wide and 30 m deep. Size gradation of blocks away from the pit is obvious on the west side. Many of the ejected blocks broke through the lava crust while the interior was still molten resulting in small squeeze-up mounds of gas-charged lava that resemble meter-scale mushrooms.

The northeast side of the field is covered with tephra blown downwind during the phreatic phase; however, numerous ejecta blocks can be found on both sides (except near Kings Bowl where vandals pushed most of the blocks into the pit). The lava field is relatively flat compared to most ESRP flows and constituted several shallow coalescent and terraced lava lakes of shelly pahoehoe representing compound lava flows. There are several places on the field where lava drained back into the fissure, merged with other flows, or forced slabs of hardened crust upward.

On the lava lake, observe the crust where it was broken while the interior was still molten. Stacks of lava crust slabs forming mounds are possibly remnants of a levee. Some cracks resulted in elongate lava squeeze-ups although circular dome-like squeeze-ups become more apparent closer to the phreatic pit. These were produced when ejecta blocks broke through the lava lake, often resulting in radial fractures, and allowed molten gas-charged lava to ooze out forming a blister of quenched lava on the surface. Some ejecta blocks can still be observed encased in the hollow protuberances.

Enter the phreatic pit from the northeast side where a walkway has been established and note the layers of fresh Kings Bowl lava covering baked soils, tephra, and underlying older ESRP lava flows. Vesicle pipes and vesicular zones extending upwards from the base of the flow suggest volatile entrainment from a moist subsurface. The lower surfaces of individual lava lobes exhibit festoon-like swirls and bulges, attributed to low viscosity flow, where they covered freshly-chilled crusts of previous lobes. Remnants of the feeder dike for the eruption (Fig. 27) can be seen at the north end of the pit where it is chilled against earlier flows.

Figure 27. The north end of Kings Bowl viewing into the fissure where remnants of the feeder dike are exposed. Access to deeper parts of the fissure is possible, although dangerous, with climbing equipment. The vertical cliff is approximately 40 m high and exposes several lava flow lobes emplaced prior to the eruption of Kings Bowl lava.

The Wapi lava field, composed of many thin overlapping pahoehoe flows (Champion, 1973; Champion and Greeley, 1977), lies ~4 km south of the Kings Bowl lava field (Fig. 23). The Wapi vents do not lie on an extension of the Kings Bowl fissures; however, a radiocarbon age of 2,270 ± 50 B.P. (Champion and Greeley, 1977; Kuntz et al., 1986b) for the Wapi system suggests that, within analytical uncertainty, the two centers are contemporaneous. Thus, the three lava fields associated with the Great Rift exhibit the highest Holocene activity of the ESRP basaltic rift systems.

Stop 11. Split Butte (Scott Hughes)

Drive 0.3 mi back to the intersection and turn left (north); then proceed 9 mi to Bear Trap Cave, a segment of a 21 km long lava tube that is an alternate stop if time permits. Bear Trap Cave is located just off the Minidoka-Arco Road. Continue south toward Minidoka approximately 4.5 mi., turn left off main road, toward Split Butte (Fig. 23). Drive along the access road toward

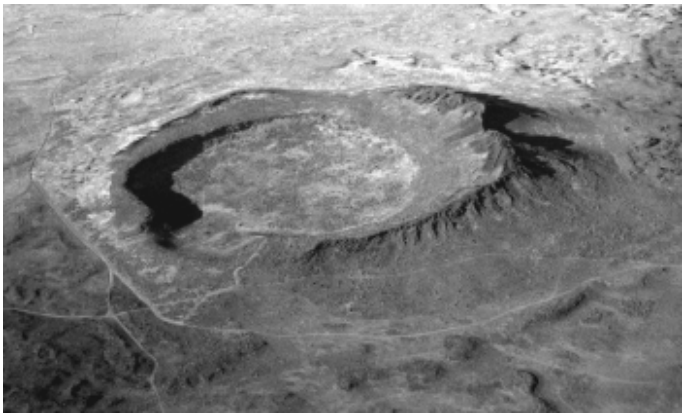

Figure 28. Split Butte looking northwest, a phreatomagmatic maar-type volcano comprised of a tephra ring and inner basalt lava lake. The lava lake partially flowed over the southwest rim and collapsed leaving a circular shelf of basalt within the crater.

the low point on the west rim of the crater and, where the break in slope prohibits driving further, continue on foot to the rim for Stop 11. Walk along the rim to observe tephra sequences then down the inner slope to the edge of the basalt cliff.

Located about one km west of the Wapi lava field, Split Butte is a maar type phreatomagmatic crater (Fig. 28) that is one of the older exposed features on the ESRP (Womer, 1977; Womer et al., 1982). The tephra ring is surrounded by loess-covered Quaternary basalts. Holocene flows from the Wapi field stopped short of lapping up on the southeast flank. The subcircular tephra ring is ~0.6 km in diameter and represents an initial eruptive phase caused by basaltic magma interacting with groundwater. A basalt lava lake, exposed as a prominent cliff within the tephra ring, indicates an effusive phase that followed construction of the ring. The inner lava lake rose to a height that was higher than the surrounding lava surface then, after minor overflow on the southwest flank, it subsided to leave a circular terrace-like platform around the inside margin of the crater. The lava lake effusive eruption was probably fairly quiet, as indicated by a lack of spatter, although slumping within the tephra ring resulted in a disconformable contact visible between it and the surrounding basalt lava.

Womer et al. (1982) point out several lines of evidence for a phreatomagmatic origin. The ash is mostly clear palagonitized sideromelane that is typically blocky and angular with few vesicles, indicating rapid quenching in a wet environment. Plastic deformation of ash layers also occurs beneath ejecta blocks, and secondary minerals such as calcite and zeolite are abundant. Pyroclastics typical of strombolian eruptions are generally absent and layers of hyaloclastite-rich coarse tephra are interspersed with fine ash having accretionary lapilli.

Drive back to the Arco-Minidoka Road, continue ~10 mi south to Minidoka and take Route 24 about 14 mi southwest to Rupert. Turn east (left) at the busy intersection onto Baseline Road, drive about 2 mi and turn south (right) and continue ~4 mi to the I-84 freeway. Proceed ~6 mi to the intersection of I-84 with I-86 and continue on I-86 ~21 mi toward Massacre Rocks State Park.

Stop 12. Massacre Volcanic Complex (Bill Hackett and Scott Hughes)

West of Pocatello, the I-86 freeway roughly parallels the Snake River along the southern physiographic boundary between Basin-and-Range and Snake River Plain geologic provinces. Late Tertiary and early Quaternary volcanic rocks partly fill the intermontane valleys of the Basin-and-Range and lap onto their adjacent mountain flanks (Trimble and Carr, 1976). Downstream from American Falls, the Snake River cuts through a complex assemblage of Pliocene basaltic tuffs and lava flows, and underlying late Miocene and early Pliocene rhyolite deposits. The Pliocene basaltic units were redefined by Luessen (1987) as the Massacre Volcanic Complex comprising the Eagle Rock, Indian Springs and Massacre Rocks basaltic pyroclastic subcomplexes, and the basalt of Rockland Valley (Fig. 29). The pyroclastic complex, which crops out over a 128 km^2 area about 15 km southwest of American Falls, was deposited during explosive phreatomagmatic eruptions along the Snake River. The Massacre Volcanic Complex overlies a sequence of unconformable volcanic and volcaniclastic deposits including (youngest to oldest) the Little Creek Formation, the Walcott Tuff, and the Neeley Formation (Fig. 30).

Continue east on I-86 freeway from Exit 21 to milepost 26 and proceed northeast to the Register Road overpass that is approximately 2 miles from Exit 28, the entrance to Massacre Rocks State Park. Stop 12A is in the roadcut on the southeast side of the

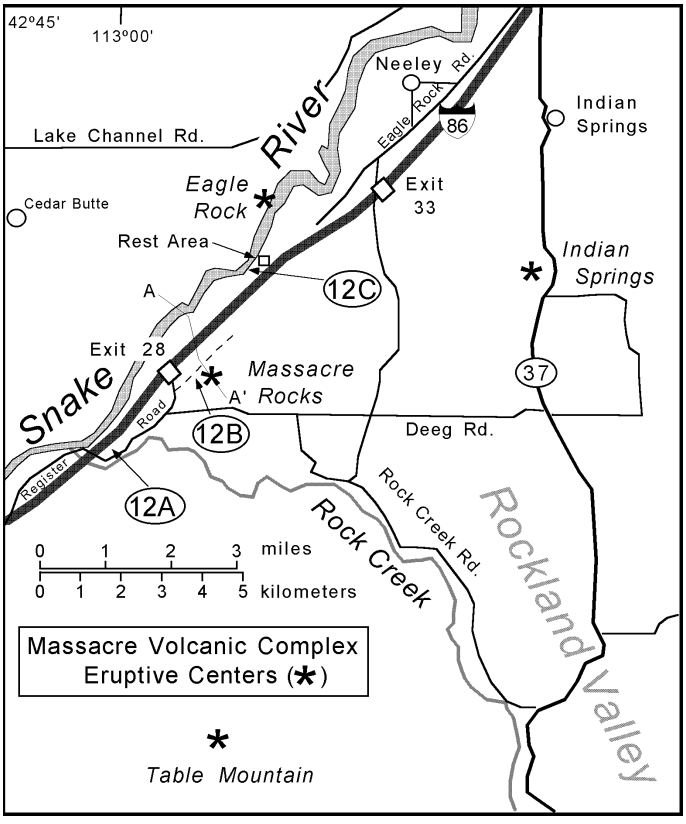

Figure 29. Map of the Massacre Rocks area with eruptive centers of the Massacre Volcanic Complex. Phreatomagmatic units of the Massacre Complex were overlain by Quaternary basalts that flowed north from eruptive centers in Rockland Valley. Field trip stops (12A - 12C) are circled.

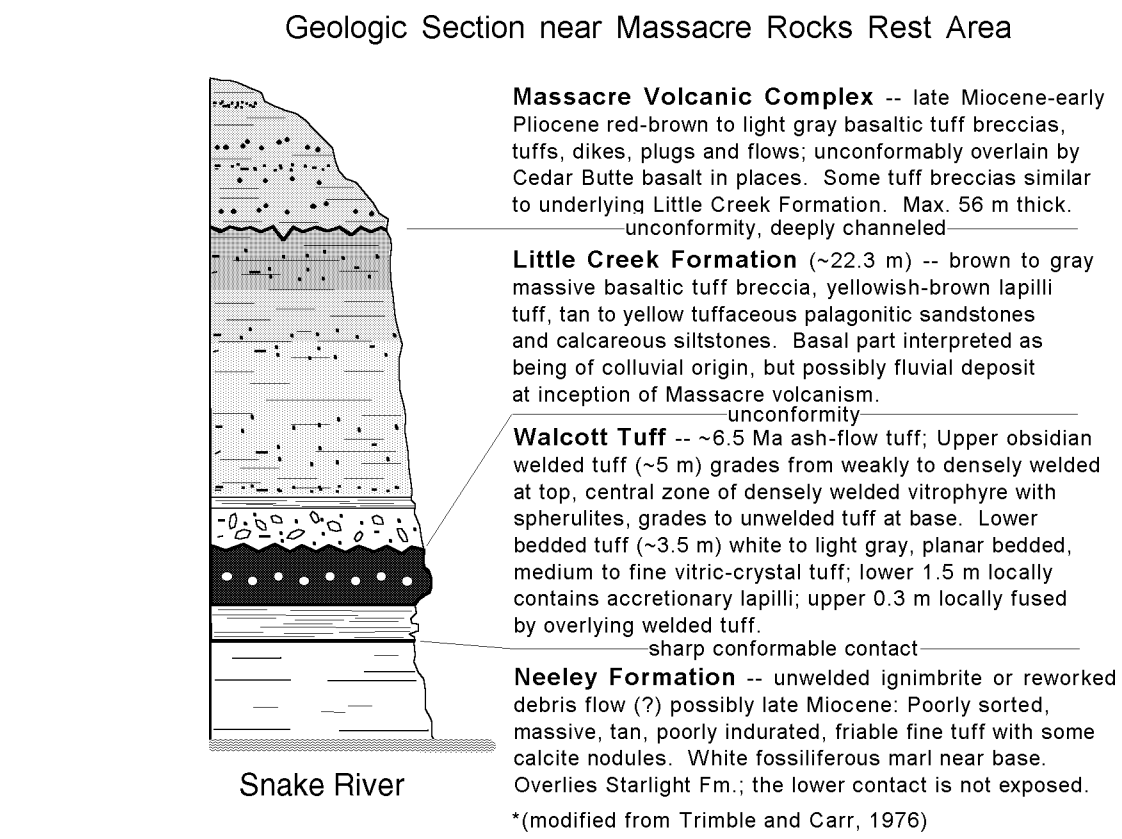

Figure 30. Geologic section at Stop 12C (access from interstate highway rest area near Massacre Rocks) illustrating sequence observed along the Snake River. Refer to Figure 29 for location of this and other stops in the Massacre Volcanic Complex. Adapted from Trimble and Carr (1976).

highway immediately past the overpass (Fig. 29). At least two subhorizontal Quaternary basalt lava flows, which flowed northward down Rockland Valley from Table Mountain shield volcano, lap onto basaltic tuffs of the Massacre Rocks subcomplex that have a slight westward dip. Autoclastic basal breccia and baked paleosol occur between the two lava flows. The underlying unit is a stratified lithic tuff with subtle gas escape features that are perpendicular to the dip. These elutriation pipes, assuming they were originally vertical, possibly indicate post-eruptive tectonic tilting or local downwarping along the southern margin of the ESRP.

Continue on the freeway and take Exit 28; turn south and then immediately northeast on the frontage road for about one-quarter mile to Stop 12B (Fig. 29) which is on juniper-covered slopes about 0.5 km south of Massacre Rocks State Park. Hike up to one of the prominences about 100 m off the road and observe bedded

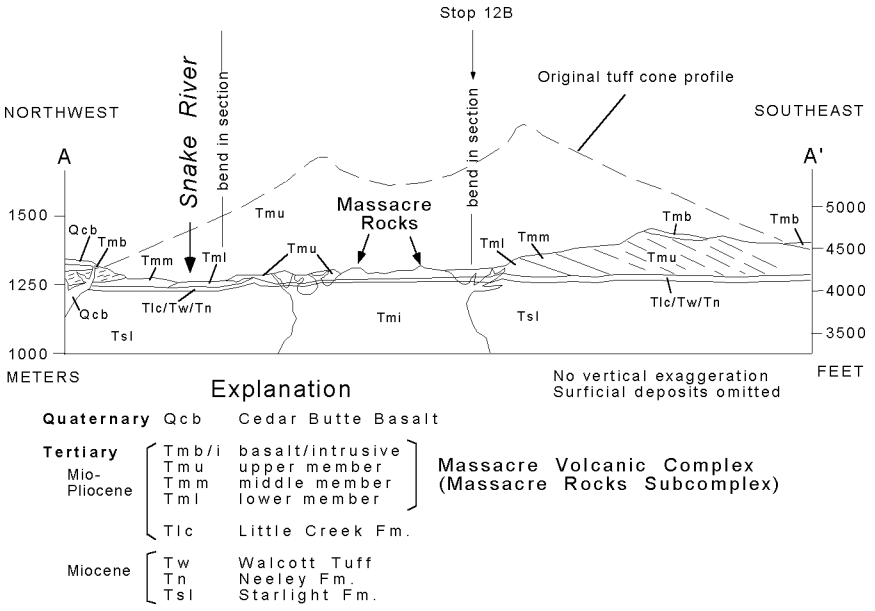

Figure 31. Geologic cross-section of the Massacre Volcanic Complex (after Luessen, 1987) through the Massacre Rocks eruptive center. Refer to Figure 29 for the location of the A-A' cross-section line.

tuff deposits and ballistic ejecta. The deposit is on the flank of the Massacre Rocks unwelded tuff cone (Fig. 31); block sags are common and reflect close proximity (less than 1 km) to the vent. Scour surfaces, well-stratified planar bedding and dunes indicate high flow velocities during volcanic surges which are fairly common in ESRP phreatomagmatic deposits.

Return to the freeway continuing northeast, take Exit 33 and re-enter the freeway headed southwest to the rest area near Massacre Rocks State Park. Walk southwest from the rest area parking lot along the paved path leading to the old Oregon Trail wagon ruts. The path forks and the paved part passes under the freeway to the Oregon Trail exhibit. Continue southwest on the unpaved path for about 100 m, leave the path and climb down the ridge toward the river to observe the stratigraphic section (Stop 12C). Figure 30 illustrates the sequence that can be observed at this location. Cedar Butte basalt, a Quaternary ESRP lava flow, and ignimbrite of the Massacre Volcanic Complex can be observed on the opposite side of the river.

Return to the freeway, drive southwest and take Exit 28, re-enter the freeway and continue northeast toward Pocatello. Pillar Butte, the primary vent area for the Holocene Wapi lava field, and the shield profile can be observed to the northwest while driving on I-86 in this region. While driving northeast through the Neeley area about 2 miles upstream from the interstate rest area, a small shield volcano and several spatter cones are visible on the north side of the river. This is a small vent area for Cedar Butte basalt (not the same petrologically-evolved Cedar Butte eruptive center described by McCurry et al., this volume), a lobe of which impounded the river and formed American Falls Lake (Carr and Trimble, 1963). The basalt lobe, ~75,000 years old, is typical ESRP lava. The lake beds are very thick near here and the lava flows have been eroded by the Bonneville Flood. Rapids in the river are caused by a fault with small displacement, possibly related to dike intrusion associated with the Cedar Butte flows.

End of field trip. Return to Pocatello via I-86 and I-15.

ACKNOWLEDGMENTS

The authors benefited from discussions, fields excursions and unselfish sharing of ideas with geologists who have worked on eastern Snake River Plain basaltic systems over the past two decades. We are especially indebted to Ron Greeley, Arizona State University; Mel Kuntz and Duane Champion, U.S. Geological Survey; Bill Leeman, Rice University; Dave Rodgers, Idaho State University; and the numerous coworkers of these individuals. Jim Riesterer and Chad Johannesen provided much-needed assistance with diagrams of lava fields. Technical reviews by Mel Kuntz, Dennis Geist, Ron Greeley, and Paul Link are greatly appreciated and significantly improved the quality of the manuscript. Much of the work reported in this guide was supported by the U.S. Department of Energy, Office of New Production Reactors and Assistant Secretary for Environmental Management, under DOE Idaho Operations Office Contract DE-AC07-94ID13223. Additional support was provided by grant #DE-FG07-96ID13420 from the U.S. Department of Energy to the Idaho Water Resources Research Institute, subcontract #KEK066-97-B to Idaho State University; and various Task Orders under EG&G, Idaho Contract C84-110421 to S. Hughes.

REFERENCES

Alt, D., Sears, J.M., and Hyndman, D.W., 1988, Terrestrial maria: The origins of large basalt plateaus, hotspot tracks and spreading ridges: Journal of Geology, v. 96, p. 647-662.

Anderson, S.R., and Bartholomay, R.C., 1995, Use of natural gamma logs and cores for determining stratigraphic relations of basalt and sediment at the Radioactive Waste Management Complex, Idaho National Engineering Laboratory, Idaho: Journal of the Idaho Academy of Science, v. 31, no. 1, p. 1-10.

Anderson, S.R., Ackerman, D.J., Liszewski, M.J., and Feiburger, R.M., 1996, Stratigraphic data for wells at and near the Idaho National Engineering Laboratory, Idaho: U.S. Geological Survey Open-File Report 96-248 (DOE/ID-22127), 27 p. and 1 diskette.

Armstrong, R.L., Leeman, W.P., and Malde, H.E., 1975, K-Ar dating, Quaternary and Neogene volcanic rocks of the Snake River Plain, Idaho: American Journal of Science, v. 275, p. 225-251.

Barraclough, J.T., and Jensen, R.G., 1976, Hydrologic data for the Idaho National Engineering Laboratory site, Idaho, 1971 to 1973: U.S. Geological Survey Open-File Report 75-526 (IDO-22060), p. 116.

Bartholomay, R.C., Orr, B.R., Liszewski, M.J., and Jensen, R.G., 1995, Hydrologic conditions and distribution of selected radiochemical and chemical constituents in water, Snake River Plain aquifer, Idaho National Engineering Laboratory, Idaho, 1989 through 1991: U.S. Geological Survey Water-Resources Investigations Report, 95-4175 (DOE/ID-22123), 47 p.

Camp, V.E., 1995, Mid-Miocene propagation of the Yellowstone mantle plume head beneath the Columbia River basalt source region: Geology, v. 23, no. 5, p. 435-438.

Carr, W.J., and Trimble, D.E., 1963, Geology of the American Falls Quadrangle, Idaho: U.S. Geological Survey Bulletin, 1121-G, 43 p.

Cecil, L.D., Orr, B.R., Norton, T., and Anderson, S.R., 1991, Formation of perched groundwater zones and concentrations of selected chemical constituents in water, Idaho National Engineering Laboratory, Idaho 1986-88: U.S. Geological Survey Water-Resources Investigations Report 91-4166 (DOE/ID-22100), 53 p.

Cerling, T.E., Poreda, R.J., and Rathburn, S.L., 1994, Cosmogenic ^{3}He and ^{21}Ne age of the Big Lost River flood, Snake River Plain, Idaho: Geology, v.22, p.227-230.

Champion, D.E., 1973, The relationship of large scale surface morphology to lava flow direction, Wapi lava field, SE Idaho [M.S. thesis]: Buffalo, State University of New York at Buffalo, 44 p.

Champion, D.E., and Greeley, R., 1977, Geology of the Wapi lava field, Snake River Plain, Idaho, *in* Greeley, R., and King, J.S., eds., Volcanism of the eastern Snake River Plain, Idaho: A Comparative planetary guidebook: Washington, D.C., National Aeronautics and Space Administration, p. 135-151.

Christiansen, R.L., and McKee, E.H., 1978, Late Cenozoic volcanic and tectonic evolution of the Great Basin and Columbia intermontane regions: Geological Society of America Memoir 152, p. 283-311.

Creighton, D.N., 1982, The geology of the Menan complex, a group of phreatomagmatic constructs in the eastern Snake River Plain, Idaho [M.S. thesis]: Buffalo, State University of New York at Buffalo, 76 p.

Creighton, D.N., 1987, Menan Buttes, southeastern Idaho, *in* Beus, S.S., ed., Centennial field guide volume 2, Rocky Mountain Section of the Geological Society of America, p. 109-111.

Eaton, G.P., and 7 others, 1975, Magma beneath Yellowstone National Park: Science, v. 188, p. 787-796.

Ferdock, G.C., 1987, Geology of the Menan volcanic complex and related features, northeastern Snake River Plain, Idaho [M.S. thesis]: Pocatello, Idaho State University, 171 p.

Fishel, M.L., 1993, The geology of uplifted rocks on Big Southern Butte: Implications for the stratigraphy and geochemistry of the Eastern Snake River Plain [M.S. thesis]: Pocatello, Idaho State University, 178 p.

Fleck, R.J., and Criss, R.E., 1985, Strontium and oxygen isotopic variations in Mesozoic and Tertiary plutons of central Idaho: Contributions to Mineralogy and Petrology, v. 90, p. 291-308.

Frederick, D.B., and Johnson, G.S., 1996, Estimation of hydraulic properties and development of a layered conceptual model of the Snake River Plain aquifer at the Idaho National Engineering Laboratory, Idaho: State of Idaho INEL Oversight Program and Idaho Water Resources Research Institute, Technical Completion Report, 67 p. and appendices.

Geist, D., and Richards, M., 1993, Origin of the Columbia Plateau and Snake River plain: Deflection of the Yellowstone plume: Geology, v. 21, p. 789-792.

Geslin, J.K., Gianniny, G.L., Link, P.K., and Riesterer, J.W., 1997, Subsurface sedimentary facies and Pleistocene stratigraphy of the northern Idaho National Engineering and Environmental Laboratory: Controls on hydrology, *in* Sharma, S., and Hardcastle, J.H., eds., Proceedings of the 32nd Symposium on Engineering Geology and Geotechnical Engineering, p. 15-28

Gianniny, G.L., Geslin, J.K., Riesterer, J., Link, P.K., and Thackray, G.D., 1997, Quaternary surficial sediments near Test Area North (TAN), northeastern Snake River Plain: An actualistic guide to aquifer characterization, *in* Sharma, S., and Hardcastle, J.H., eds., Proceedings of the 32nd Symposium on Engineering Geology and Geotechnical Engineering, p. 29-44.

Greeley, R., 1977, Basaltic "plains" volcanism, *in* Greeley, R., and King, J.S., eds., Volcanism of the eastern Snake River Plain, Idaho: A Comparative planetary guidebook: Washington, D.C., National Aeronautics and Space Administration, p. 23-44.

Greeley, R., 1982, The Snake River Plain, Idaho: Representative of a new category of volcanism: Journal of Geophysical Research, v. 87, p. 2705-2712.

Greeley, R., and King, J.S., 1977, eds., Volcanism of the eastern Snake River Plain, Idaho: A Comparative planetary guidebook: Washington, D.C., National Aeronautics and Space Administration, 308 p.

Greeley, R., Theilig, E., and King, J.S., 1977, Guide to the geology of Kings Bowl lava field, *in* Greeley, R., and King, J.S., eds., Volcanism of the eastern Snake River Plain, Idaho: A comparative planetary guidebook: Washington, D.C., National Aeronautics and Space Administration, p. 171-188.

Hackett, W.R., and Morgan, L.A., 1988, Explosive basaltic and rhyolitic volcanism of the eastern Snake River Plain, *in* Link, P.K., and Hackett, W.R., eds., Guidebook to the Geology of Central and Southern Idaho: Idaho Geological Survey Bulletin 27, p. 283-301.

Hackett, W.R., and Smith, R.P., 1992, Quaternary volcanism, tectonics, and sedimentation in the Idaho National Engineering Laboratory area, *in* Wilson, J.R., ed., Field Guide to Geologic Excursions in Utah and Adjacent areas of Nevada, Idaho, and Wyoming: Utah Geological Survey, Miscellaneous Publication 92-3, p. 1-18.

Hackett, W.R., and Smith, R.P., 1994, Volcanic hazards of the Idaho National Engineering Laboratory and adjacent areas: U.S. Department of Energy, Idaho National Engineering Laboratory Document INEL-94/0276, 31 p.

Hamilton, W.B., 1989, Crustal geologic processes of the United States, *in* Pakiser, L.C., and Mooney, W.D., Geophysical framework of the continental United States: Geological Society of America Memoir 172, p. 743-781.

Hayden, K.P., 1992, The geology and petrology of Cedar Butte, Bingham County, Idaho [M.S. thesis]: Pocatello, Idaho State University, 104 p.

Hildreth, W., Halliday, A. N., and Christiansen, R. L., 1991, Genesis and contamination of basaltic and rhyolitic magma beneath the Yellowstone Plateau volcanic field: Journal of Petrology, v. 32, p. 63-138.

Hon, K., Kauahihaua, J., Denlinger, R., and McKay, K., 1994, Emplacement and inflation of pahoehoe sheet flows: observations and measurements of active lava flows on Kilauea Volcano, Hawaii: Geological Society of America Bulletin, v. 106, p. 351-370.

Hughes, S.S., Casper, J.L., and Geist, D.J., 1997a, Potential influence of volcanic constructs on hydrogeology beneath Test Area North, Idaho National Engineering and Environmental Laboratory, Idaho, *in* Sharma, S., and Hardcastle, J.H., eds., Proceedings of the 32nd Symposium on Engineering Geology and Geotechnical Engineering, p. 59-74.

Hughes S.S., Wetmore, P.H., and Casper, J.L., 1997b, Geochemical interpretations of basalt stratigraphy and Quaternary mafic volcanism, eastern Snake River Plain, Idaho: Geological Society of America Abstracts With Programs, v. 29, no. 7, p. A-298.

Hughes S.S., Smith, R.P., Hackett, W.R., McCurry, M., Anderson, S.R., and Ferdock, G.C., 1997c, Bimodal magmatism, basaltic volcanic styles, tectonics, and geomorphic processes of the eastern Snake River Plain, Idaho, *in* Link, P.K. and Kowallis, B.J., eds., Proterozoic to Recent Stratigraphy, Tectonics, and Volcanology, Utah, Nevada, Southern Idaho and Central Mexico, Geological Society of America Field Trip Guidebook, Brigham Young University Geology Studies, vol. 42, part 1, p. 423-458.

Hughes S.S., Wetmore, P.H., and Casper, J.L., in press, Evolution of Quaternary tholeiitic basalt eruptive centers on the eastern Snake River Plain, Idaho, *in* Bonnichsen, B., White, C.M., eds., Tectonic and magmatic evolution of the Snake River Plain volcanic province: Idaho Geological Survey.

Keszthelyi, L., and Denlinger, R., 1996, The initial cooling of pahoehoe flow lobes: Bulletin of Volcanology, v. 58, p. 5-18.

Knobel, L.L., Cecil, L.D., and Wood, T.R., 1995, Chemical composition of selected core samples, Idaho National Engineering Laboratory, Idaho: U. S. Geological Survey Open-File Report 95-748, 59 p.

Kuntz, M.A., 1979, Geologic map of the Juniper Buttes area, eastern Snake River Plain, Idaho: U.S. Geological Survey Miscellaneous Investigations Series, Map I-1115, 1:48,000.

Kuntz, M.A., 1989, Geology of the Craters of the Moon Lava Field, Idaho: Field Trip Guidebook T305, American Geophysical Union, p. 51-61.

Kuntz, M.A., 1992, A model-based perspective of basaltic volcanism, eastern Snake River Plain, Idaho, *in* Link, P. K., Kuntz, M. A., and Platt, L. P., eds., Regional geology of eastern Idaho and western Wyoming: Geological Society of America Memoir 179, p. 289-304.

Kuntz, M.A., and Dalrymple, G.B., 1979, Geology, geochronology, and potential volcanic hazards in the Lava Ridge-Hell's Half Acre area, eastern Snake River Plain, Idaho, U.S. Geological Survey Open-File Report 79-1657, 70 p.

Kuntz, M.A., Dalrymple, G.B., Champion, D.E., and Doherty, D.J., 1980, Petrography, age, and paleomagnetism of volcanic rocks at Radioactive Waste Management Complex, Idaho National Engineering Laboratory, Idaho, with an evaluation of volcanic hazards: U.S. Geological Survey Open File Report 80-388, 63 p.

Kuntz, M.A., Champion, D.E., Spiker, E.C., Lefebvre, R.H., and McBroome, L.A., 1982, The Great Rift and the evolution of the Craters of the Moon lava field, Idaho, *in* Bonnichsen, Bill, and Breckenridge, R.M., eds., Cenozoic Geology of Idaho: Idaho Bureau of Mines and Geology Bulletin 26, p. 423-438.

Kuntz, M.A., Champion, D.E., Spiker, E.C., and Lefebvre, R.H., 1986a, Contrasting magma types and steady-state, volume-predictable volcanism along the Great Rift, Idaho: Geological Society of America Bulletin, v. 97, p. 579-594.

Kuntz, M.A., Spiker, E.C., Rubin, M., Champion, D.E., Lefebvre, R.H., 1986b, Radiocarbon studies of latest Pleistocene and Holocene lava flows of the Snake River Plain, Idaho; data, lessons, interpretations: Quaternary Research, v. 25, p. 163-176.

Kuntz, M.A., Champion, D.E., Lefebvre, R.H., and Covington, H.R., 1988, Geologic map of the Craters of the Moon, Kings Bowl, Wapi lava fields and the Great Rift volcanic rift zone, south-central Idaho: U. S. Geological Survey Miscellaneous Investigation Series Map I-1632, scale 1:100,000.

Kuntz, M.A., Covington, H. R., and Schorr, L. J., 1992, An overview of basaltic volcanism of the eastern Snake River Plain, Idaho, *in* Link, P. K., Kuntz, M. A., and Platt, L. P., eds., Regional geology of eastern Idaho and western Wyoming: Geological Society of America Memoir 179, p. 227-267.

Kuntz, M.A., Skipp, B., Lanphere, M.A., Scott, W.E., Pierce, K.L., Dalrymple, G.B., Champion, D.E., Embree, G.F., Page, W.R., Morgan, L.A., Smith, R.P., Hackett, W.R., and Rodgers, D.W., 1994, Geologic map of the Idaho National Engineering Laboratory and adjoining areas, eastern Idaho: U.S. Geological Survey Miscellaneous Investigations Series Map 1-2330, scale 1:100,000.

Lanphere, M.A., Kuntz, M.A., and Champion, D.E., 1994, Petrography, age, and paleomagnetism of basaltic lava flows in coreholes at Test Area North (TAN), Idaho National Engineering Laboratory, U.S. Geological Survey Open-File Report 94-686, 49 p.

Leeman, W.P., 1982a, Development of the Snake River Plain—Yellowstone Plateau province, Idaho and Wyoming: An overview and petrologic model, *in* Bonnichsen, Bill, and Breckenridge, R.M., eds., Cenozoic Geology of Idaho, Idaho Bureau of Mines and Geology Bulletin 26, p. 155-177.

Leeman, W.P., 1982b, Evolved and hybrid lavas from the Snake River Plain, Idaho, *in* Bonnichsen, Bill, and Breckenridge, R.M., eds., Cenozoic Geology of Idaho, Idaho Bureau of Mines and Geology Bulletin 26, p. 193-202.

Leeman, W.P., 1982c, Evolved and hybrid lavas from the Snake River Plain, Idaho, *in* Bonnichsen, Bill, and Breckenridge, R.M., eds., Cenozoic Geology of Idaho, Idaho Bureau of Mines and Geology Bulletin 26, p. 193-202.

Leeman, W.P., Vitaliano, C.J., and Prinz, M., 1976, Evolved lavas from the Snake River Plain, Craters of the Moon National Monument, Idaho: Contributions to Mineralogy and Petrology, v. 56, p. 35-60.

Leeman, W.P., Menzies, M.A., Matty, D.J., and Embree, G. F., 1985, Strontium, neodymium, and lead isotopic compositions of deep crustal xenoliths from the Snake River Plain: evidence for Archean basement: Earth and Planetary Science Letters, v. 75, p. 354-368.

Link, P.K., and Phoenix, E.C., 1996, Rocks Rails & Trails, 2nd Edition, Idaho Museum of Natural History, 194 p.

Luessen, M.J., 1987, Geology of Massacre Volcanic Complex, eastern Snake River Plain, Idaho. [M.S. thesis]: Pocatello, Idaho State University, 163 p.

Malde, H.E., 1991, Quaternary geology and structural history of the Snake River Plain, Idaho and Oregon, *in* Morrison, R.B., ed., Quaternary nonglacial geology; Conterminous U.S.: Boulder, Colorado, Geological Society of America, The Geology of North America, v. K-2, p. 251-281.

Manga, M., 1995, Waves of bubbles in basaltic magmas and lavas: Journal of Geophysical Research, vol. 101, No. B8, p. 17,457 - 17,465.

McCurry, M., Hackett, W.H., and Hayden, K., 1999, Cedar Butte and cogenetic Quaternary rhyolite domes of the eastern Snake River Plain, *in* Hughes, S.S., and Thackray, G.D., eds., Guidebook to the Geology of Eastern Idaho, Idaho Museum of Natural History, this volume

McCurry, M., Bonnichsen, B., White, C., Godchaux, M.M., and Hughes, S.S., 1997, Bimodal basalt-rhyolite magmatism in the central and western Snake River Plain, Idaho and Oregon, *in* Link, P.K. and Kowallis, B.J., eds., Proterozoic to Recent Stratigraphy, Tectonics, and Volcanology, Utah, Nevada, Southern Idaho and Central Mexico, Geological Society of America Field Trip Guidebook, Brigham Young University Geology Studies, vol. 42, part 1, p. 381-422.

Morin, R.H., Barrash, W., Paillet, F.L., and Taylor, T.A., 1993, Geophysical logging studies in the Snake River Plain aquifer at the Idaho National Engineering Laboratory – wells 44, 45, and 46: U.S. Geological Survey Water-Resources Investigations Report 92-4184, 44 p.

Morin-Jansen, A., 1987, Study of the principle lineament and associated lineaments [M.S. thesis]: Pocatello, Idaho State University, 79 p.

Morgan, W.J., 1972, Plate motions and deep mantle convection: Geological Society of America Memoir 132, p. 7-22.

Muller, O.H., and Pollard, D.D., 1977, The stress state near Spanish Peaks, Colorado, determination from a dike pattern: Pure and Applied Geophysics, v. 115, p. 69-86.

Myers, W.B., and Hamilton, W., 1964, Deformation accompanying the Hebgen Lake earthquake of August 17, 1959: U.S. Geological Survey Professional Paper 435, p. 55-98.

Olsen, G.L., 1996, Soil erosion results: Interdepartmental Communication #GLO-01-96, Lockheed-Martin Idaho Technologies Company, 5 p.

Pierce, K.L. and Morgan, L.A., 1992, The track of the Yellowstone hotspot: Volcanism, faulting, and uplift, *in* Link, P.K., Kuntz, M.A., and Platt, L.P., eds., Regional geology of eastern Idaho and western Wyoming: Geological Society of America Memoir 179, p. 1-53.

Pierce, K.L., Fosberg, M.A., Scott, W.E., Lewis, G.C., and Coleman, S.M., 1982, Loess deposits of southeastern Idaho: age and correlation of the upper two loess units, *in* Bonnichsen, Bill, and Breckenridge, R.M., eds., Cenozoic Geology of Idaho, Idaho Bureau of Mines and Geology Bulletin 26, p. 717-725.

Pollard, D.D., Delaney, P.T., Duffield, W.A., Endo, E.T., and Okamura, A.T., 1983, Surface deformation in volcanic rift zones: Tectonophysics, v.94, p.541-584.

Prinz, M., 1970, Idaho rift system, Snake River Plain, Idaho: Geological Society of America Bulletin, v. 81, p. 941-947.

Rathburn, S.L., 1991, Quaternary channel changes and paleoflooding along the Big Lost River, Idaho National Engineering Laboratory: Idaho National Engineering Laboratory Informal Report EGG-WM-9909, 33 p.

Rathburn, S.L., 1993, Pleistocene cataclysmic flooding along the Big Lost River, east central Idaho: Geomorphology, v.8, p. 305-319.

Reed, M.F., Bartholomay, R.C., and Hughes, S.S., 1997, Geochemistry and stratigraphic correlation of basalt lavas beneath the Idaho Chemical Processing Plant, Idaho National Engineering Laboratory: Environmental Geology, v. 30, p. 108-118.

Richards, M.A., Duncan, R.A., and Courtillot, V.E., 1989, Flood basalts and hot spot tracks: Plume heads and tails: Science, v. 246, p. 103-107.

Rodgers, D.W., Hackett, W.R., and Ore, H.T., 1990, Extension of the Yellowstone Plateau, eastern Snake River Plain, and Owyhee Plateau: Geology, v. 18, 1138-1141.

Rubin, A.M., 1992, Dike-induced faulting and graben subsidence in volcanic rift zones: Journal of Geophysical Research, v. 97, no. B2, p. 1839-1858.

Rubin, A.M., and Pollard, D.D., 1987, Origins of blade-like dikes in volcanic rift zones: U.S. Geological Survey Professional Paper 1350, Chapter 53, p. 1449-1470.

Rubin, A.M., and Pollard, D.D., 1988, Dike-induced faulting in rift zones of Iceland and Afar: Geology, v.16, p.413-417.

Scott, W.E., 1982, Surficial geologic map of the eastern Snake River Plain and adjacent areas, Idaho and Wyoming: U. S. Geological Survey Miscellaneous Investigation Map I-1372, scale 1:250,000.

Smith, R.B., and Sbar, N.L., 1974, Contemporary tectonics and seismicity of the western United States with emphasis on the Intermountain Seismic Belt: Geological Society of America Bulletin, v. 85, p. 1205-1218.

Smith, R. B., and Braile, L. W., 1994, The Yellowstone hotspot: Journal of Volcanology and Geothermal Research, v. 61, p. 121-187.

Smith, R.P., Hackett, W.R., and Rodgers, D.W., 1989, Geological aspects of seismic hazards assessments at the INEL, southeastern Idaho: Proceedings of the Second DOE Natural Hazards Mitigation Conference, Knoxville, Tennessee, p. 282-289.

Smith, R.P., Jackson, S.M., and Hackett, W.R., 1996, Paleoseismology and seismic hazards evaluations in extensional volcanic terrains: Journal of Geophysical Research, v. 101, no. B3, p.6277-6292.

Spear, D.B., 1979, The geology and volcanic history of the Big Southern Butte-East Butte area, eastern Snake River Plain, Idaho [Ph.D. Dissertation]: State University of New York at Buffalo, 136 p.

Spear, D.B., and King, J.S., 1982, The geology of Big Southern Butte, Idaho, *in* Bonnichsen, Bill, and Breckenridge, R. M., eds., Cenozoic Geology of Idaho, Idaho Bureau of Mines and Geology Bulletin 26, p. 395-403.

Stearns, H.T., Crandall, L., and Steward, W.G., 1938, Geology and groundwater resources of the Snake River Plain in Southeastern Idaho: U.S. Geological Survey Water Supply Paper 774, 268 p.

Stout, M.Z., and Nicholls, J., 1977, Mineralogy and petrology of Quaternary lava from the Snake River Plain, Idaho: Canadian Journal of Earth Sciences, v. 14, p. 2140-2156.

Stout, M.Z., Nicholls, J., and Kuntz, M.A., 1994, Petrological and mineralogical variations in 2500-2000 yr B.P. lava flows, Craters of the Moon lava field, Idaho: Journal of Petrology, v. 35, p. 1682-1715.

Trimble, D.E., and Carr, W.J., 1976, Geology of the Rockland and Arbon Quadrangles, Power County, Idaho: U.S. Geological Survey Bulletin 1399, 115 p.

Welhan, J., Funderberg, T., Smith, R.P., and Wylie, A., 1997, Stochastic modeling of hydraulic conductivity in the Snake River Plain Aquifer: 1. Geologic constraints and conceptual approach, *in* Sharma, S., and Hardcastle, J.H., eds., Proceedings of the 32nd Symposium on Engineering Geology and Geotechnical Engineering, p. 75-91.

Welhan J.A., Johannesen, C.M., Glover, J.A., Davis, L.L., and Reeves, K.S., in press, Overview and synthesis of lithologic controls on aquifer heterogeneity in the eastern Snake River Plain, Idaho, *in* Bonnichsen, B., White, C.M., eds., Tectonic and magmatic evolution of the Snake River Plain volcanic province: Idaho Geological Survey.

Wetmore, P.H., 1998, An assessment of physical volcanology and tectonics of the central eastern Snake River Plain based on the correlation of subsurface basalts at and near the Idaho National Engineering and Environmental Laboratory, Idaho [M.S. thesis]: Pocatello, Idaho State University, 79 p

Wetmore, P.H., Hughes, S.S., Anderson, S.R., 1997, Model morphologies of subsurface Quaternary basalts as evidence for a decrease in the magnitude of basaltic magmatism at the Idaho National Engineering and Environmental Laboratory, Idaho, *in* Sharma, S., and Hardcastle, J.H., eds., Proceedings of the 32nd Symposium on Engineering Geology and Geotechnical Engineering, p. 45-58.

Womer, M.B., 1977, The origin of Split Butte, a maar type crater of the south-central Snake River Plain, Idaho, *in* Greeley, R., and King, J.S., eds., Volcanism of the eastern Snake River Plain, Idaho: A Comparative planetary guidebook: Washington, D.C., National Aeronautics and Space Administration, p. 190-202.

Womer, M.B., Greeley, R., and King, J.S., 1982, Phreatic eruptions of the eastern Snake River Plain of Idaho, *in* Bonnichsen, Bill and Breckenridge, R.M., eds., Cenozoic Geology of Idaho: Idaho Bureau of Mines and Geology Bulletin 26, p. 453-464.